LIFETIME PREDICTION OF POLYMERS IN NUCLEAR POWER PLANTS 2022

RAPPORT 2023:960

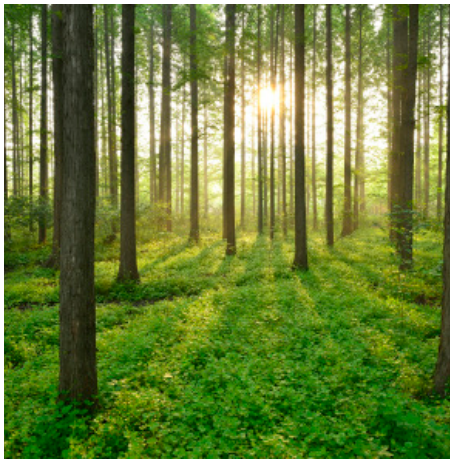

POLYMERA MATERIAL I KÄRNKRAFTSTILLÄMPNINGAR

Energiforsk

Lifetime prediction of polymers in nuclear power plants 2022

Improved material management by combining traditional ageing and sensitive analysing techniques.

ANNA BONDESON, HENRIK TOSS, MOHIT PUSHP AND DAVID KIEFER

ISBN 978-91-7673-980-0 | © Energiforsk november 2023

Energiforsk AB | Telefon: 08-677 25 30 | E-post: kontakt@energiforsk.se | www.energiforsk.se

Foreword

Since most Swedish and Finnish nuclear power plants now are in long term operation, i.e., past the original planned lifetime of the plants, the safe long-term use of polymer components and improving their ageing management is critical. Safety criteria assessment and ageing management needs to be at sufficient level in order to prevent premature component breakdown and avoiding endangering the overall safety.

This report summarizes results from the SAMPO project that has been running for four years. The acronym SAMPO stands for Safety criteria and improved ageing management research for polymer components exposed to thermal-radiative environments. The project has been studying ageing mechanisms in thermal-radiative environments, determining how to set acceptance criterion properly and providing robust tools for condition monitoring.

The Nordic nuclear industry has cooperated on polymer research through the Finnish nuclear safety R&D program SAFIR for several years. Detailed results are found in task deliveries from the project, available on the Energiforsk web under the Polymers in nuclear applications program page.

Project leader has been senior researcher Konsta Sipilä from VTT, the Swedish part including this report has been made by Anna Bondesson et al RISE. The activities are financed by the SAFIR program, The Swedish Radiation Safety Authority and Vattenfall, Uniper/Sydkraft Nuclear, TVO, Fortum, Skellefteå Kraft and Karlstads Energi through the Polymers in nuclear applications program.

Sammanfattning

SAMPO var ett samarbetsprojekt i samarbete med VTT i Finland och RISE och drevs i nära samarbete med kärnkraftsindustrin. Polymerforskare arbetade tillsammans med experter inom sensorteknik och känsliga analystekniker för att öka kunskapen om hur plast- och gummimaterial bryts ned under lång tids användning i kärnkraftverk. Syftet var att fastställa relevanta acceptanskriterier för komponenternas livslängd och förbättrad materialhantering genom användning av t.ex. online-övervakning av material.

Projektet innehöll en serie workshops med alla nordiska kärnkraftverk för att identifiera och välja lämpliga och relevanta polymerkomponenter. I synnerhet identifierades tätningar och O-ringar som intressanta komponenter att studera, med potential att öka utbytesintervallet. Det är viktigt med relevanta acceptanskriterier och i fallet med O-ringar är det relevant att studera deras deformation, dvs. "kompressionssättning" när den är monterad i ventiler etc. och jämföra med procentuell deformation vid läckage. Materialegenskaper jämfördes med läckagetester i specialdesignade testriggar. En jämförelse mellan tre kvaliteter av EPDM för O-ringar utfördes vilket visade på stor skillnad i prestanda med ålder. Två överlägsna kvaliteter hade höga värden på sättningen, över 90% innan vattenläckage observerades. Traditionellt används 80% sättning som slutet av livslängden för O-ringar men ett högre värde kan användas och utbytesintervall kan omvärderas.

En uppsättning olika polymera komponenter som membran, kablar och bjälklagstätningar mottogs från kärnkraftverk och referensmaterial anskaffades där det var möjligt. Livstidsanalyser utfördes på referensmaterial och jämfördes med statusen för de komponenter som hämtades från anläggningarna. När det gäller ventilmembran uppvisade de stor spridning i materialegenskaper beroende på position och olika användningsförhållanden.

Permittivitet är en egenskap som är möjlig att mäta på polymerer online, utan provuttag eller förstöra produkten. Det är därför en attraktiv metod för att övervaka materialnedbrytning och återstående livslängd online. Flera olika mätutrustningar användes för att studera åldrandet av gummiprover.

Isotermisk mikrokalorimetri undersöktes som ett verktyg för att studera termisk nedbrytning närmare de verkliga temperaturerna som 50, 60 ° C eller högre (maximalt 150 ° C). Tekniken användes för att beräkna aktiveringsenergi för nedbrytning av EPDM-gummi med och utan antioxidanter och för att studera material uttagna från ett kärnkraftverk.

Keywords

Acceptance criteria, NPP, rubber, sealings, O-rings, polymer ageing, permittivity, antenna technology, micro-calorimetry

Acceptanskriterier, Kärnkraftverk, gummi, o-ringar, polymer åldring, permittivitet, antennteknologi, mikrokalorimetri

Summary

SAMPO was a joint project in collaboration with VTT in Finland and RISE and did run in close collaboration with the nuclear industry. Polymer researchers worked together with experts in sensor technology and sensitive analysis techniques to learn more about the degradation of plastics and rubber materials used for long periods of time in Nuclear Power plants. The objectives were to set relevant acceptance criteria for the end-of-life of components, and improved material management by use of e.g., online monitoring of materials.

The project contained a series of workshops with all Nordic nuclear power plants to identify and chose suitable and relevant polymer components. In particular, sealings and O-rings were identified as interesting components to study, with the potential to increase the interval of exchange. Relevant acceptance criteria are essential and in the case of O-rings, it is relevant to study their deformation i.e., "compression set" when mounted in valves, etc., and compare to the degree of deformation to leakage. Material properties were compared to leak tests in specially designed test rigs. A comparison between three grades of EPDM for O-rings was performed indicating a large difference in performance with age. Two superior grades had a high level of compression set, above 90% before water leakage was observed. Traditionally 80% set is used as end-of-life for O-rings, but a higher value could be used, and exchange intervals may be re-evaluated.

A set of different polymer components such as membranes, cables, and joist seals were received from nuclear power plants and reference material was procured where possible. Lifetime analyses were performed on reference materials and compared with the status of the components retrieved from the plants. In the case of valve membranes, a large difference in terms of their properties was found as a result of different service conditions.

Permittivity is a property possible to measure on polymers online, without sample outtake or destroying the product. It is therefore an attractive method to monitor material degradation and residual service life online. A range of different measurement equipment was used to study the aging of rubber samples.

Isothermal microcalorimetry was investigated as a tool to study thermal degradation closer to real-life temperatures such as 50, 60 °C, or higher (maximum 150 °C). The technique was used to calculate activation energy for the degradation of EPDM rubber with and without antioxidants and to study materials received directly from a nuclear power plant.

Content

1 About the SAMPO project

The interest in polymer ageing issues has increased nationally and internationally as the original planned lifetime of NPPs is about to be reached and extended lifetime is desired.

Since polymers are used in numerous different applications within NPPs and each polymer type can have different compositions depending on its use, a vast amount of unique polymer blends which contribute to the overall safety of the plants needs to be managed. Thus, it becomes essential to identify the most important topics among so many components and phenomena that contribute to the overall safety of the plants. To do this identification, a collaborative group between experts from Finnish and Swedish plant operators, regulators and researchers was established during the last SAFIR-program period. The group is interacting with each other to identify the most relevant topics in NPP polymer component research and as an outcome, the most relevant topics relate to sufficient acceptance criteria and safety margin assessments and reliable ageing management procedures.

SAMPO was funded by the SAFIR-program of the Finnish State Nuclear Waste Management Fund (VYR) and some of the research performed at RISE was funded by Energiforsk and Strålsäkerhetsmyndigheten (SSM). SAMPO is a continuation of the COMRADE project run between 2016 and 2019.

In this report there is some repetition of results from previous reports to allow reading this report alone.

2 Objective

The main objective of the project was to produce data and techniques that should help to improve the overall safety of NPPs by more precise evaluation methods for degradation behaviour of polymer materials. The aim was to provide improved acceptance criteria and safety margin assessment as well as by enhancing ageing management.

The project aimed to result in the following developments:

Case studies of several components after their service in nuclear power plants, their total lifetime based on analysis of suitable reference materials and improved safety margin assessment for a critical polymer component.

Verification of isothermal microcalorimetry as a potential technique to study aging and lifetime of polymers.

Improve ageing management via enhanced condition monitoring techniques such as online measurements of dielectric properties.

3 Plan and implementation of the project

The SAMPO (Safety criteria and improved ageing management research for polymer components exposed to thermal radiative environment) project was a joint project with the Finnish research institute VTT and the Swedish RISE. SAMPO started in 2019 and was running until January 2023. It was divided into different work packages and four of them are laid out in more detail in the following parts.

This report represents the work that RISE was responsible for. Following tasks were lead by RISE.

T1.1 was to make use of the results and analyses from the COMRADE project when suggesting new acceptance criteria and safety margins. Results from laboratory ageing tests and evaluations have been compared to materials obtained from NPPs

T1.3 aimed to attain usage lifetimes for rubber O-rings which are present in critical functional capacities in Nuclear Powerplants (NPPs). A focus was put on utilising model materials to attain material failure, further verifying methods, and better representing average power plant material.

T2.1 aimed to evaluate if ageing behaviour of the polymer materials could be tracked online by using dielectric and by broad band frequency mapping of the dielectric behaviour of the materials under test.

T2.2, purpose of this study was to investigate, if microcalorimeter can be used as a complementary technique to the widely accepted ATA (Accelerated Thermal Ageing), to predict service lifetime of polymer materials. To be able to measure changes in the material properties before and after accelerated thermal ageing rather high exposure temperatures are necessary.

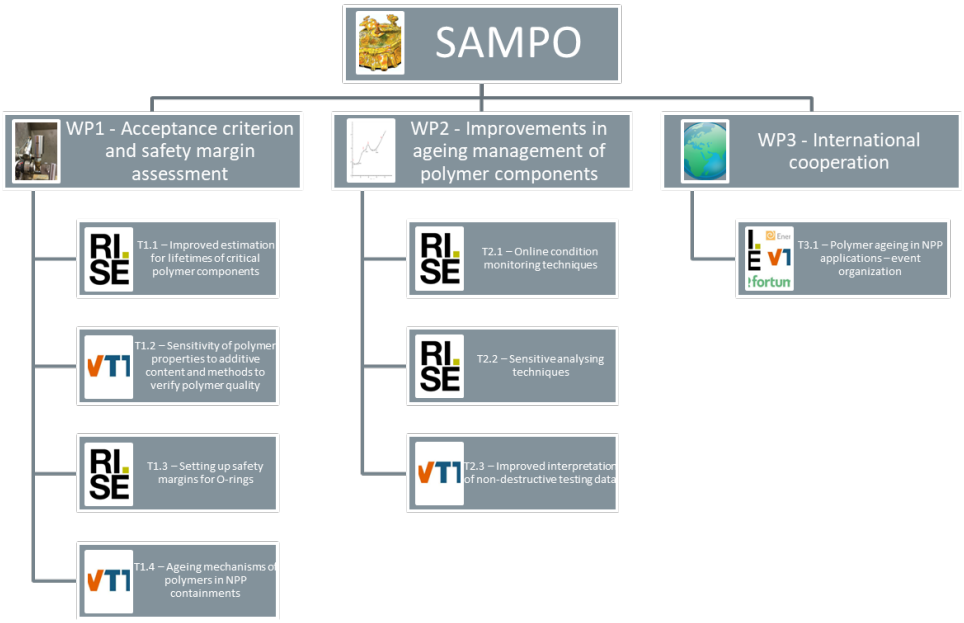

Figure 1. Work packages of the SAMPO project (2019-2023)

4 Acceptance criteria and Safety margins for O-rings used in NPPs

4.1 BACKGROUND AND AIM

This task aimed to attain usage lifetimes for rubber O-rings which are present in critical functional capacities in Nuclear Powerplants (NPPs). A focus was put on utilising model materials to attain material failure, further verifying methods, and better representing average power plant material.

Rubber O-rings can be found in some critical components such as pumps and pipe connections. If these pipes were to fail, a so-called 'loss of coolant accident' (LOCA) could occur. This could obviously be disastrous to the Powerplant and surroundings.

This project aims to verify the results from previous research project (Sipilä, Jansson et al. 2018), where nuclear grade polymer rubbers were tested. In this project we will use same test methods as in Comrade but with lower quality grade rubber materials, this to obtain quicker results.

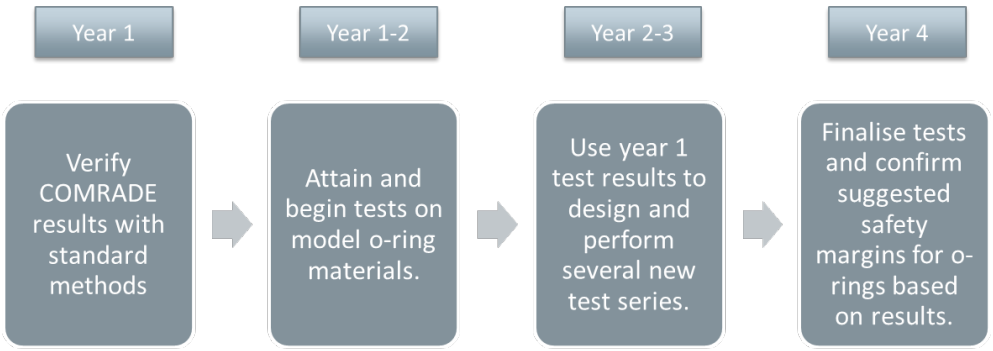

Figure 2. Plan for SAMPO Task 1.3

4.2 EXPERIMENTAL

4.2.1 Materials

Ethylene Propylene Diene Monomer (EPDM) is a common material used in sealing rings in nuclear applications since EPDM is resistant to radiation. The materials used in the project was kindly supplied by James Walker Ltd. Three grades are used during this project listed in Table 1. Grade 1 has previously been used in COMRADE and SAMPO 2019, and grade 2 is a bespoke material fabricated from James Walker for SAMPO. Grade 3 EPDM is an off-the-shelf consumer grade EPDM. Figure 3 shows the TGA (thermogravimetric analysis) results for the 3 different grades of EPDM where you can see the difference in composition of binder (polymer and plasticizing oil evaporates between 50-600 °C in N_2), carbon black (burns at 600 °C in O_2) and the residue of inorganic fillers.

Table 1. EPDM grades investigated in project.

Grade	Type	Number
1	Nuclear	LR9444
2	Industrial	LR9678
3	Consumer, stabilized	NA

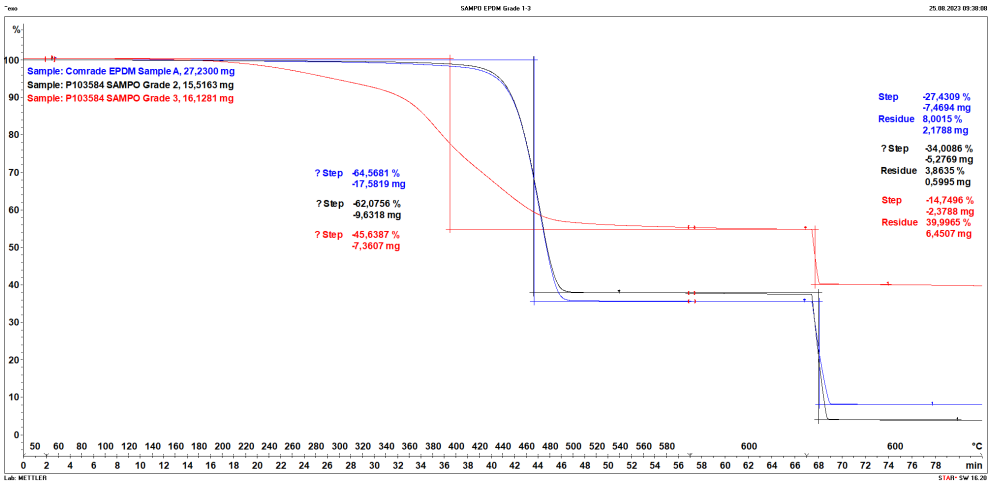

Figure 3. TGA curves of EPDM Grade 1 (blue), 2 (black) and 3 (red).

4.2.2 Compression set and Stress relaxation tests

Compression set is a standard test method (ISO 815-1) used to evaluate sealing performance of rubber materials. Either a cylindrical test piece or an O-ring may be analysed. The bolts were tightened so that the percentage of the compression was 75% of the original thickness. In total, three assembled compression devices were papered for EPDM and nitrile sample, respectively.
The compression was performed in air and was calculated as:

$$\frac{h_0 - h_1}{h_0 - h_s} \times 100\% \qquad (1)$$

where h_0, h_1 and h_s is the initial thickness of test specimen, the thickness of the test specimen after recovery, and height of the spacer, respectively.

Leak test rigs had O-rings compressed to approximately 20 % and calculated as above.

Stress relaxation testing was performed in duplicate for each temperature (90, 120, 140 °C). The method is similar to compression set but instead of measuring deformation of the test after exposure, the counterforce is continuously measured. When the test piece is compressed, the elastic rubber causes a counter force that can be measured. The samples were compressed initially to 75 % and the force was measured continuously until 50 % of initial force was reached (test of samples in 90 °C was discontinued before reaching 50 %).

4.3 RESULTS AND DISCUSSION

4.3.1 Compression set and leak tests

The initial work focused on the overall verification of the data attained in the prior project COMRADE, i.e., the method used in COMRADE (measurement on O-rings), and the standardised method for measuring compression set (cylindrical cut-outs from a sheet) (Sipilä, Jansson et al. 2018). This experimentation showed that the data is reliable in both circumstances. Further on the compression set of a model material provided by James Walker (JW), at a level which has been described by JW as 6/10 (denoted grade 2 material), where the material (grade 1) measured previously is considered at top levels, 9-10/10. The purpose of this was two-fold. Firstly, we wanted to assure that a material could reach failure, unlike the prior COMRADE project, where the top-level material was used, and failure was rare – thus casting into doubt at time whether the experiment was at fault, or if the material was simply very high quality. Secondly, it is unknown whether power plants will at all times use top level material, so experimentation upon a more realistic, yet still proficient material, was deemed wise.

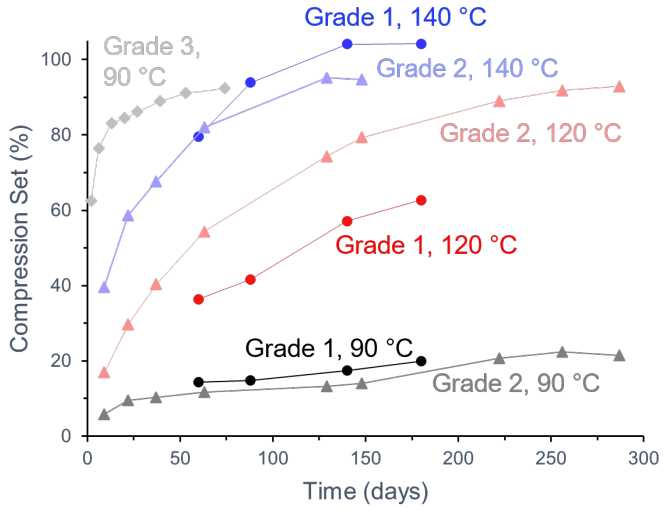

Figure 4. Comparison of compression set of EPDM grades 1 and 2 at 90 120 and 140 °C, as well as grade 3 at 90 °C. An activation energy of ~100 and ~103 kJ/mol was estimated by time-temperature superposion for grade 1 and 2, respectively.

Compression set of grade 1 EPDM material previously measured in the COMRADE project and compression set of grade 2 material are depicted in Figure 4 (Sipilä, Jansson et al. 2018). At 120 °C one can observe the grade 2 material performing worse than the top-level grade 1 material, with, as far as the data goes, ~60 vs. ~85 % respectively. Therefore, it is expected that grade 2 material will likely reach failure even during leak testing despite similar activation energies. The activation energy for grade 1 material is likely underestimated as only aging at 140 °C has reached the end-of-life criteria of 80 % compression set (Burnay, S. 2018).

Experimentation also involved compression set within leak test rigs, to simulate realistic working conditions. During a symposium summarising 2019 data for stakeholders, it was brought to our attention that the 'old' test rigs may not be deemed satisfactory enough for duplicating the environment that O-rings find themselves in inside a power plant. Thus, the rigs were redesigned as per Figure 5, where one can see

a groove has been cut out for the ring to sit within, compared to the 'old' test rig with much more empty space in the centre.

Figure 5. O-ring test rigs. Left: old test rig from COMRADE. Right: new test rig re-designed for SAMPO.

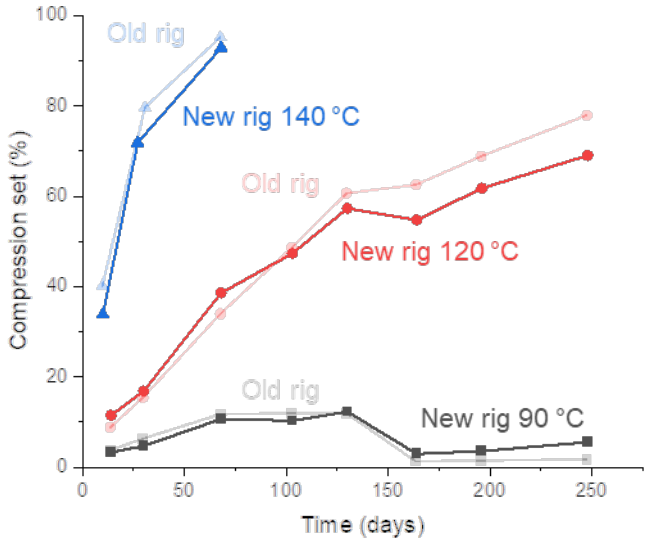

Figure 6. Compression set of grade 2 EPDM O-rings with 'old' and 'new' redesigned test rigs at 90, 120 and 140 °C.

Compression set measurements have been performed for EPDM material within both leak test rig designs, and the data can be found in Figure 6. The data follows the expected trend, with raising temperature, a higher compression set is attained. Leak testing has been performed at several time points, no leaks were detected except for the 'old' rig, at 140 °C. For the first of the two time points a leak was detected under low pressure (~5 Bar) and once the operating pressure for the test was attained (~60 Bar), the leak was no longer detected. It could be deduced that the higher pressure allowed the O-ring to attain a tighter seal within the test rig. For the last point at 140 °C, the rig

was leaking continuously and could not hold any higher pressure. No leak was detected for series at 120 and 90 °C.

Both grade 1 and 2 materials are high quality EPDM grades which is clearly visible in the previous results. Since it cannot be excluded that besides special high quality grade also lower quality material may be used for O-rings in nuclear power plants a third grade of lower quality EPDM was added to the analysis. Since it was not known how quickly and at what temperatures this grade would show changes in its compression set a first set of data at 50, 90 and 120 °C was collected. No significant compression set at 50 °C was recorded while at 120 °C measurements turned out to be likely difficult due to diffusion limited oxidation. However, the series at 90 °C showed an expected trend of continuously rising compression set with aging time. A second series at 70, 80, and 90 C° was recorded (Figure 7). Aging affects the compression set of grade 3 much more significantly than the other grades as can be seen in Figure 4 when comparing the data for 90 °C. The grade 3 samples reaches compression set of 80 % after only about 15 days at 90 °C, compared to both grade 2 and 3 which do not reach this value within the experimental time.

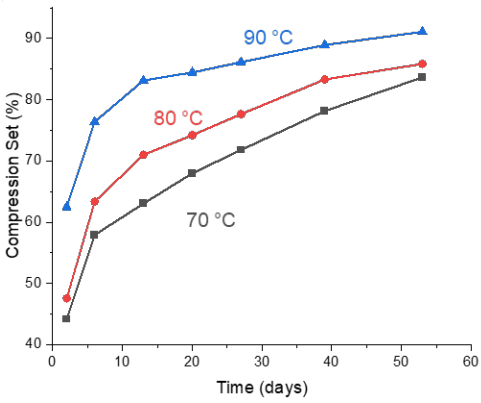

Figure 7. Compression set of grade 3 material after aging at 70, 80, and 90 °C. We estimate an activation energy E_a of ~75 kJ/mol.

4.3.2 Stress relaxation test

Stress relaxation was conducted to determine the time to critical degradation value (F_{50}, 50% compression) for all EPDM material grades (Figure 8 and Table 2). For grade 1 and 2 samples were aged under compression at 90, 120 and 140 °C. As expected, aging at 140 °C resulted in the fastest decay of the compression force and both samples reached the critical value after 45 and 17 days for grade 1 and grade 2, respectively. Instead, at 120 °C grade 2 reached the critical value after 112 days. Grade 1 did not reach the critical value within the experimental time. Instead, the time to the critical value was extrapolated to about 193 days. At 90°C neither grade 1 nor grade 2 reached the critical value within the experimental time. (ISO 3384-1)

The stress relaxation of grade 3 was measured at 80, 90 and 100 °C. To compare this grade with the other two grades the expected time to the critical value at 120 and 140 °C was extrapolated to 0.3 and 0.1 days, respectively, using activation energy. Thus grade 3 shows significantly faster degradation also during stress relaxation as compared with grade 2 and 3.

Table 2. Time for F_{50}, the critical value, at 50% compression from two sample average. ([a]Material was aged at this temperature but did not reach F_{50} within the time of the experiment. [b] Calculated value. [c] One cylindrical sample and one O-ring were used for analysis.)

Temperature	Grade 1	Grade 2	Grade 3
	Time to F_{50} [days]		
80 °C	-	-	9,9
90 °C	-[a]	-[a]	3.7
100 °C	-	-	1.6
120 °C	193[a][b]	112	0.3[b]
140 °C	45[c]	19	0.1[b]

Overall, the industrial EPDM rubber (grade 2) performs somewhat below that of the nuclear EPDM rubber (grade 1). Both grades should be suitable to be used in NPP's with grade 2 requiring somewhat higher exchange intervals. Instead, a commercial EPDM rubber (grade 3) should not be used due to its low performance. The current exchange intervals for O-rings in NPP's are not known to the authors. However, based on exchange intervals of other components they are likely to be within the range of 3-8 years. Depending on the environment and temperature EPDM O-rings of similar quality to grade 1 and 2 the exchange intervals may be adjusted depending on what EPDM O-rings are being used. Safety margins for grade 1 may be somewhat larger than for grade 2 O-rings.

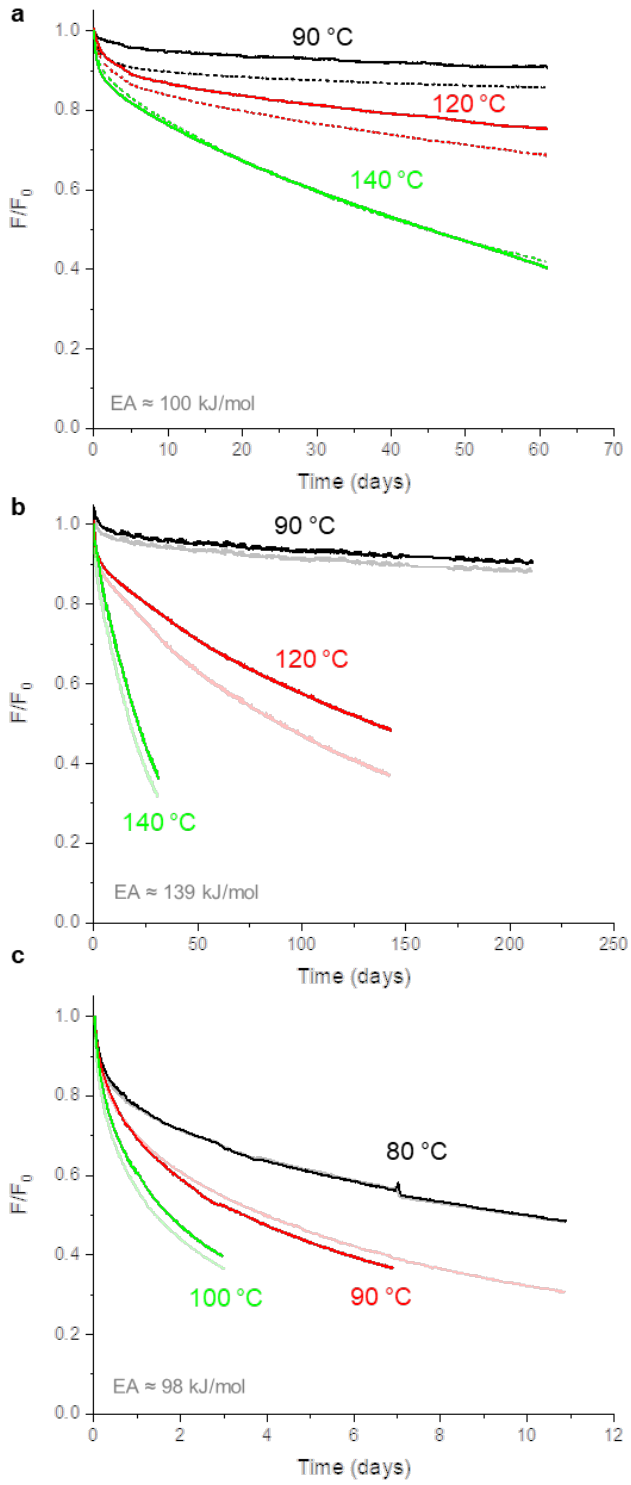

Figure 8. Stress relaxation of (a) grade 1, (b) grade 2 and (c) grade 3 EPDM material. For grade 1: Bold and dashed lines correspond to cylindrical test pieces and O-rings, respectively. For grade 2 and 3 tests were performed twice with cylindrical test pieces. Note, that the estimated activation energies for grade 1 and 2 may be somewhat erroneous since not all curves reached the critical value.

4.4 CONCLUSIONS

Three different EPDM grades for O-rings were tested using compression set and stress relaxation. As expected, the top-level grade 1 for nuclear applications performed best overall, followed by grade 2 for industrial applications. Instead, the commercial grade 3 performed significantly lower. Leak test performed showed that both grades 1 and 2 do not leak unless aged at high temperature (140°) for a long duration. Grade 2 is likely to represent the average of O-rings used in NPPs and despite a somewhat lower performance may be sufficient with suitable service intervals. Overall, it is shown that three different EPDM grades have significantly different lifetimes and thus care should be taken when choosing EPDM components for safety critical infrastructure like NPPs.

5 Improved estimation of service life of critical polymer components

5.1 BACKGROUND AND AIM

This task made use of the results and analyses from the completed COMRADE project when suggesting useful and relevant acceptance criteria and safety margins. Results from laboratory aging tests and evaluations have been compared to materials obtained from Nuclear Powerplants (NPPs). (Sipilä, Jansson et al. 2018) Improvements to both test methods and aging environments are required to define more relevant acceptance criteria as well as safety margins. Some polymer components are extremely complicated or impossible to change in operating NPPs and thus their endurance during the whole lifetime of a plant is essential. To be able to make reliable lifetime estimations of components, information on material properties on both materials that have been in use at NPPs, and artificially aged materials is extremely valuable. The question of residual lifetime assessment of polymer components in service is often raised. Without sufficient material data and service history of the materials, i.e., temperature, radiation dose, oxygen, and moisture content in the atmosphere, this is almost impossible to predict. By studying materials from NPPs available from outages and decommissioned plants that have been in service for a long time, we employed material lifetime prediction methods with correlation to materials from real service environment and long-term use.

The aim of this task was to identify critical components and to investigate the possibilities to obtain such components from plants under decommissioning or during maintenance, including material data. An obstacle with getting interesting components from decommissioning of NPPs, such as Ringhals R2 which were closed December 31, 2019, and Ringhals R1 which were closed December 31, 2020, was that it was not possible to obtain the materials for several years because the fuel was not be removed from the reactor immediately.

It was difficult to get clearance of materials used in the NPPs and was sometimes also difficult to procure sufficient amounts of materials to perform relevant tests, therefore a full year project including workshops together with the NPPs was planned for this task to discuss what components to choose. In COMRADE many samples were too small and not in sufficient amount to be analysed. Therefore, artificially aged materials were investigated in parallel. This work package was run in collaboration with micro-calorimetry (MC) tests in order to calculate activation energies and verify the MC technology. (Sipilä, Jansson et al. 2018)

5.2 PROJECT PLAN

The work package task followed the plan below:

1) Identification of critical components in all plants

2) Possibility to extraction the components from plants

3) Estimating their residual and total lifetime.

4) If possible, order samples made from the same material from the supplier

METHODS

The workshops that were held at Ringhals NPP and Forsmark NPP were used to identify critical and interesting materials for further investigating. In a first stage focus was set on Ringhals because of the upcoming decommission of two reactors but during the decommissioning time it was not possible to attain materials because critical components were still in use in the reactors.

Discussion of materials of special interest for the project were also held at the SAMPO workshop at Fortum, Espoo in November 27-28th 2019. ("Polymers in nuclear applications (2019)", Conference)

Testing was performed by using traditional mechanical methods such as tensile testing, compression set and hardness. In addition, microcalorimetry (MC) was used as an attempt to find a sensitive method to analyse status of degradation in a material. The MC method allows use of small material quantities and analyses chemical reactions in samples which either evolve energy, like exothermal oxidative degradation reactions or endothermic reactions which consumes energy.

5.3 RESULTS AND DISCUSSION

5.3.1 Selected materials for testing

EPDM O-rings were selected as a special point for interest, as these materials are easy to obtain and may be compared to the tested materials for verifying results in COMRADE WP1 and SAMPO WP1.3. They are common in the NPPs and are regularly replaced. But due to the small sample size many O-rings needed to be collected to get a statistically relevant data set. We received several EPDM-O-rings (5.0x246) after their service life at Ringhals and reference O-rings of the same type.

Neoprene membranes from Ringhals NPP were collected from earlier revisions. The collection contains several membranes of similar type and from similar conditions and time-in-use.
- Outtake was made in September 2018
- They have been in the plant for 8 years (which is maintenance interval)
- There is membranes of three dimensions 40, 19 and 17.5 cm in diameter

Reinforced EPDM seal between structure joists from TVO
- Installed in 2005, planned lifetime until 2025
- Exposure temperature 45 °C, during power operation in nitrogen atmosphere, after outage it has been stored in air
- Installed in L-shape
- Should withstand LOCA, the LOCA profile would be some time at 2,4 bar and 95°C followed by some time at 3,7 bar and 170°C

Only a small amount of material and no reference material was available for analysis.

Cables with CPE (Chlorinated Polyethylene) jacket and EPR (Ethylene propylene rubber) isolation were received from Forsmark NPP. The cables were in service for about 30 years at the NPP. A reference cable of similar type was procured.

5.3.2 Test program

EPDM O-rings

- Compression set (120, 140 °C).
- Stress-strain characteristic in compression (90, 120, 140 °C).
- Tensile properties (aging at 120 and 140°C).
- Hardness (aging at 120 and 140°C).
- LOCA test was excluded in year 3 of the project due to missing relevance for the component.

Neoprene membranes

- Tensile properties (aged at 70, 90, 110 °C).
- Hardness (aged at 70, 90, 110 °C).
- LOCA test were excluded in year 3 of the project due to missing relevance for the component.

EPDM joint seal

- Tensile properties: the material from TVO was aged at 120 °C for 45 days.
- Due to the small amount of material no further testing could be performed.

CPE cables

- Tensile properties aged at 90, 100, 110 °C (dry and soaked in oil).
- Hardness aged at 90, 100, 110 °C (dry and soaked in oil).

5.3.3 Test methods and specimen preparation

Reinforced rubber materials (membranes and joist seal) were split to remove the reinforcing material and specimen were punched from the resulting rubber sheets.
Tensile testing was made according to ISO 37 with type 2 dumbbell on a Zwick Z1 tensile tester at a rate of 500mm/min and with a clip-on extensometer.
The hardness was measured according to ISO 48-2 on a Bareiss Digitest Hardness Tester equipped with an IRHD-m measuring device.
Compression set was measured according to ISO 815 with type B cylindrical test pieces using 25% compression of the original thickness. Specimen thickness was measured using a micrometre gauge.
Stress-strain characteristic in compression (stress relaxation) was performed according to ISO 3384 with O-rings or same specimens as were used for compression set.

5.3.4 Results from testing

EPDM O-rings

Several EPDM O-rings, both used as well as new reference were received from Ringhals. The exact service conditions for the used O-rings were not known. It is assumed that these O-rings were subjected to moderate service temperatures.

Figure 9. O-rings delivered from Ringhals NPP.

For the reference samples the overall lifetime was evaluated by measuring the stress relaxation under compression at several temperatures (Figure 10). A common end-of-life criteria for compression set is when F/F_0 reaches 0.5. (ref) For aging at 140 and 150 °C this value is reached after ~1000 and ~600 hours, respectively. Instead, for 90 and 120 °C the drop of the initial force progresses significantly slower, and the experiments were terminated after 140 days. Time-temperature superposition fitting of the stress relaxation curves allowed us to extract an activation energy of ~98.1 kJ/mol. Extrapolation of the time required to reach a stress relaxation of 0.5 at 25 °C yields an extremely long theoretical lifetime. This indicates a relatively high quality of the EPDM rubber.

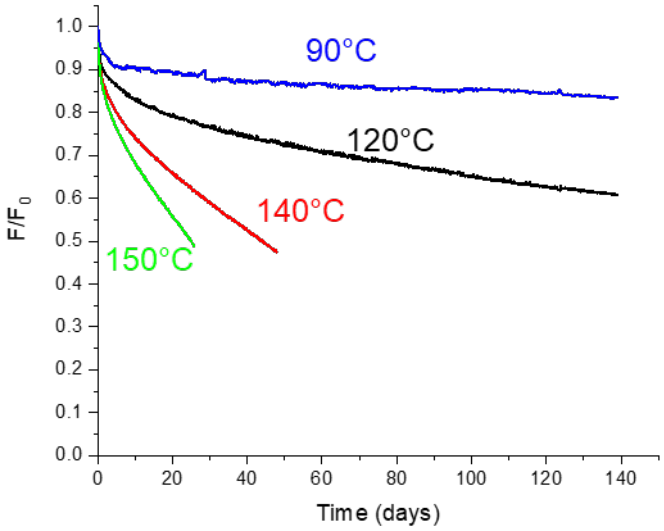

Figure 10. Stress relaxation under compression for unused O-rings from Ringhals at 90, 120, 140 and 150 °C.

The compression set and hardness of reference O-rings was measured for samples aged at 120 and 140 °C (Figure 11). The compression set of the samples at 120 °C increased from an initial ~20% after 9 days to ~50% after 200 days. Instead, aging at 140 °C increased from ~37% to ~90% after only 100 days. The m-IRHD hardness increased for the same time periods from ~80 to ~85 and ~90 for aging at 120 and 140 °C, respectively. For O-rings a compression set of 80% is often used as end-of-life criterium, which is reached after about 80 days aging at 120 °C. (Burnay,S. 2018)
Moreover, the tensile properties of the O-rings were measured. O-rings had an initial elongation at break of 80%, which decreased to ~20% after aging for just above 100 days at 140 °C. Instead, the elongation at break decreased to ~50 % for after aging for 200 days at 120 °C. For O-rings tensile stress is usually not very high as their compression properties are more relevant for their application.
Both the hardness and elongation at break was measured for four O-rings received from Ringhals after their service life. Compression set was not tested on the used O-rings from Ringhals because the unknown but likely long time passing from dismounting to test had made the material relax to an extent that would make it hard to correlate the results to the compression set made on reference O-rings. The results were compared with those O-rings heat aged at 120 and 140°C. All four O-rings from Ringhals have a similar hardness as unaged O-rings which may indicate that they are hardly affected by their service life. This finding correlates very well with the extrapolation of the theoretical lifetime indicating a good quality of the O-ring. Instead, the elongation at break of the O-rings from Ringhals is spread between 60 and 90 % with large error bars. However, elongation at break is usually less relevant in the context of O-rings and no further conclusions may be drawn.
Overall, based on the results it may be possible to increase the service time for the O-rings. However, further characterization and more specific environmental data are necessary to provide a more precise answer to whether longer service times may be suitable.

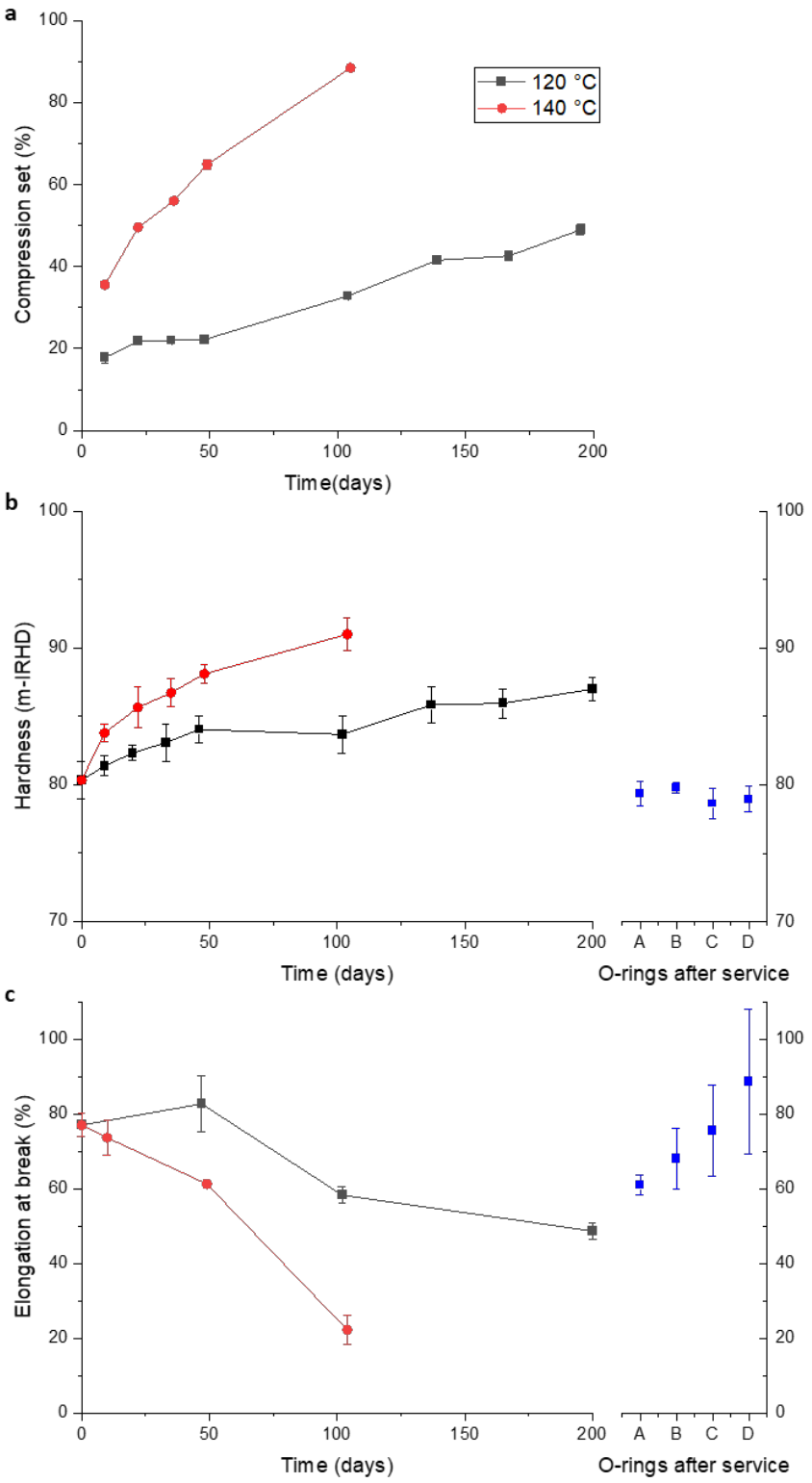

Figure 11. Compression set (a), hardness (b) and elongation at break (c) of O-rings aged at 120 and 140 °C and hardness and elongation at break of O-rings after service at Ringhals NPP. (Lines are guides to the eye.)

Neoprene membranes

Several neoprene membranes were received from outtakes at Ringhals NPP. All membranes were in service for 8 years exposed to air at ambient, but the exact service conditions for each for individual sample is unknown. Two types of membranes with diameters 17.5 and 19.0 cm were investigated. Additionally, five pristine reference membranes (19.0 cm) were received from Ringhals NPP storage (Figure 12). Reference samples for the smaller membranes were not available, but TGA analysis indicates that both membranes are of similar type.

Figure 12. Photograph of new neoprene membranes from Ringhals NPP.

To evaluate the overall lifetime of the neoprene membranes we chose to age reference membranes at 70, 90, and 110 °C and follow the tensile properties and hardness. The tensile strength and elongation at break are plotted in Figure 13a and b. The materials tensile strength is affected by aging to a low degree until long aging time when a sudden drop is noted for high temperatures. This is a common behaviour for rubber samples. Instead, elongation at break is more suitable to follow the aging. For 70 °C a slow decay of the elongation at break with aging time and more drastic changes for 90 and 110°C is noted. In Figure 13c the hardness of the sample with aging is displayed, showing a slow increase in hardness with aging time for 70 °C. Instead, aging at 110 °C degrees lead to a steep increase in hardness.

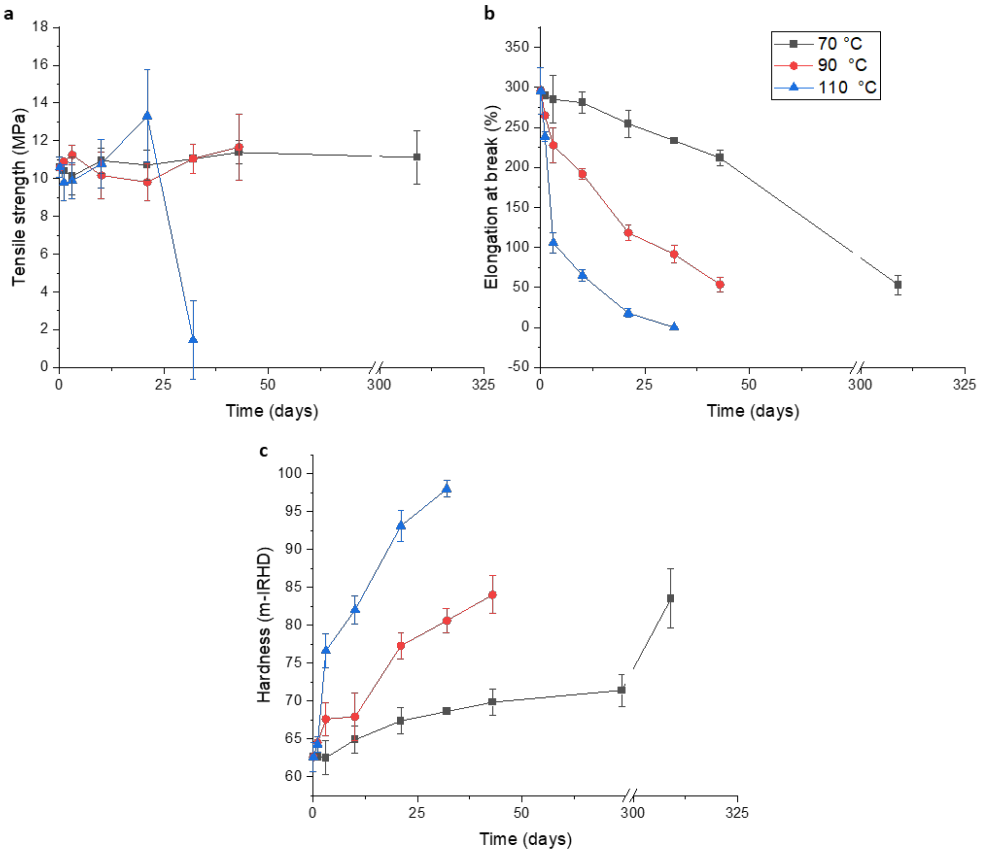

Figure 13. Tensile strength (a), elongation at break (b) and hardness (c) of heat-aged membranes from Ringhals NPP.

The datasets from elongation at break and hardness was used to build time-temperature superposition plots by shifting the x-axis of the curves to fit one master curve. The time-temperature superposition master curve for elongation at break data is shown in Figure 14a. By confirming that the trends from different temperatures are in line with each other it can be assumed that the same mechanism governs aging for all temperatures. Fitted shift factors were used to estimate the activation energy (Ea) of the aging process using Arrhenius equation for both elongation at break (see Figure 14b) and hardness. Results are listed in Table 4. For both elongation at break similar shift factors and hence a similar Ea of around 98 kJ/mol were calculated. (ISO 11346)
The shift factors and master curve were used to extrapolate the aging behaviour to an ambient temperature of 25°C allowing to estimate the total expected lifetime of the material at this temperature (Figure 14c). A common end-of-life criteria for the elongation at break is a 50% reduction corresponding to an elongation at break of around 150 % in case of the analysed neoprene samples (dashed blue horizontal line). (Buranay, S. 2018) Based on the accelerated thermal aging analysis this end-of-life criteria would be reached after approximately 35 years at 25 °C.

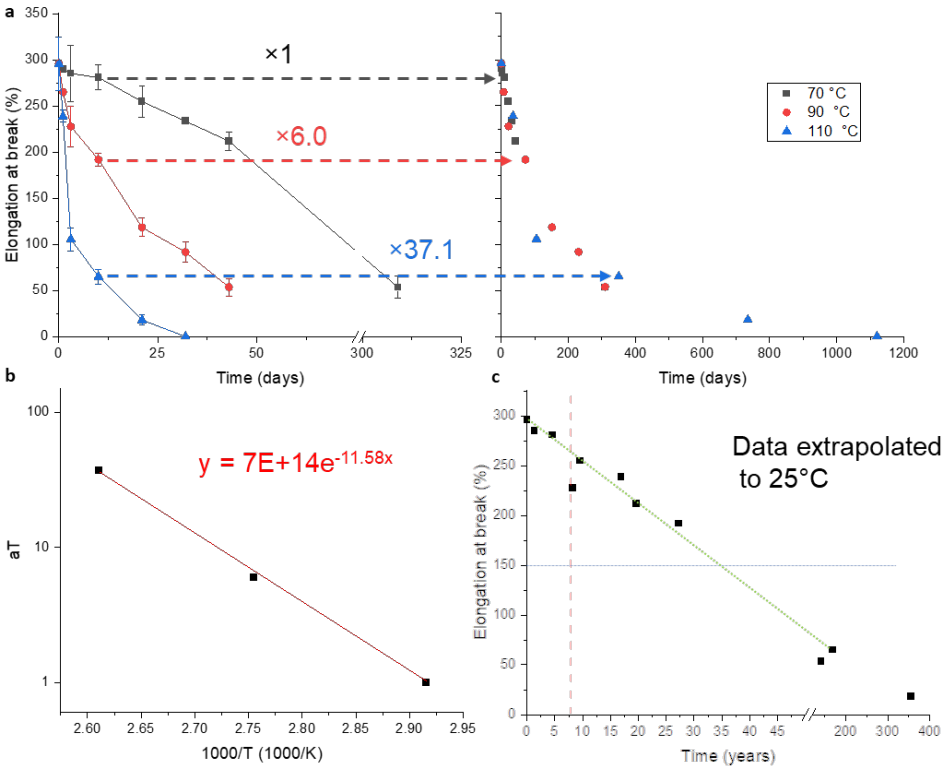

Figure 14. (a) Time-temperature superposition of elongation at break data, (b) Arrhenius fit to shift factors (aT), and (c) elongation at break data extrapolated to 25 °C (Lines are guides to the eye.).

Table 3. Shift factors (aT) and activation energies (Ea) for elongation at break and hardness.

Temperature (°C)	aT – Elongation at break	aT – Hardness
70	1	1
90	6.0	6.5
110	37.1	37.2
E_a (kJ/mol)	98.6	98.7

The tensile properties and hardness of membranes with a diameter of 19.0 cm after 8 years of service are shown in Figure 15. The elongation at break and hardness of all membranes are within the interval 260 – 290 % and 63 – 68 m-IHRD. A good agreement with the extrapolated master curve for elongation at break in Figure 14c (red dashed line) with the samples from Ringhals is noted. Based on this analysis much of the service-life of the membranes remains when membranes are exchanged every 8 years. Depending on what end-of-life criteria may be used the exchange interval may be doubled or even further increased. Note, however, that this analysis does not consider mechanical loads during operation, nor aging of the reinforcement material.
An overall good correlation between the elongation at break and hardness of the material was found. Thus, hardness measurements may potentially be used as non-destructive method to estimate the remaining service life. For example, a 50% reduction of elongation at break correlates with an m-IRHD hardness in the interval of 70 – 75. A disadvantage with hardness measurements is the small scale available, which is why similar microindenter method is often used instead. Note, that further studies would be

necessary to confirm the correlation between elongation at break and m-IRHD hardness.

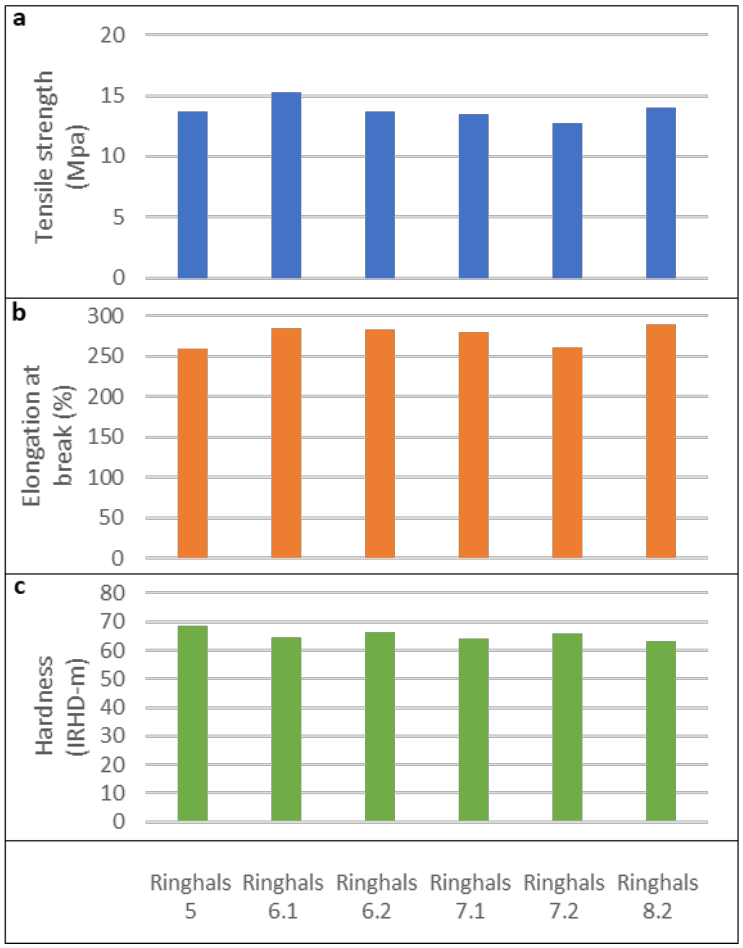

Figure 15. Tensile strength (a), elongation at break (b) and hardness (c) of neoprene membranes with a diameter of 19.0 cm as received from Ringhals NPP.

Analysis of membranes with a diameter of 17.5 cm is limited due to missing reference samples. TGA analysis (Figure 16) of the different (Ø 19.0 and 17.5 cm) membranes received revealed slightly different material compositions allowing only limited comparison. Tensile properties and hardness of membranes with Ø 17.5 shown in Figure 17 differ strongly between samples. Four of the samples have strongly reduced elongation at break below 100. Instead, three samples have an elongation at break well above 200 %. Unfortunately, the initial values are unknown, but a similar value as for Ø 19.0 membranes may be assumed. It is unknown, if the wide spread of properties reflects different conditions during service life since the exact conditions per sample could not be provided. Also, for Ø 17.5 cm membranes a low elongation at break seam to correlate with a higher hardness.

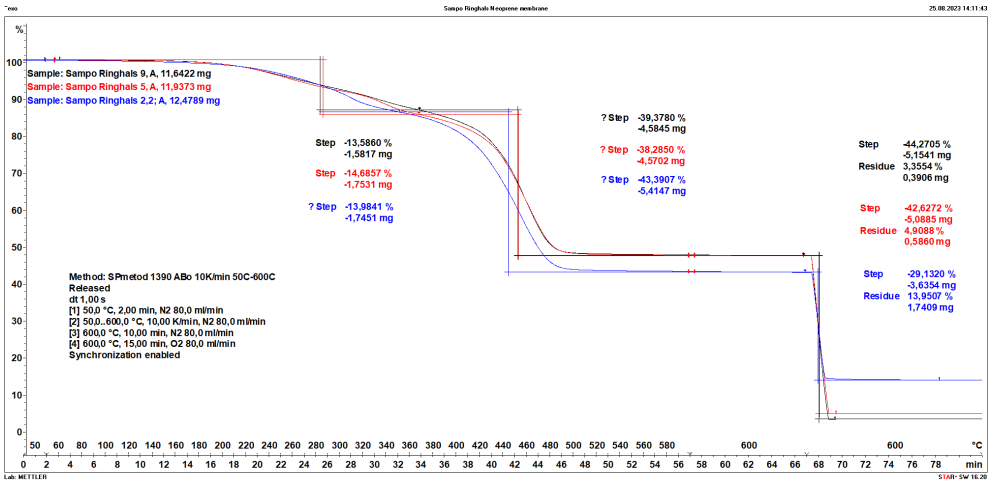

Figure 16. TGA curves for examples of three membranes, with designation 2.2, 5 and 9 (not tested.

An estimation of maximum lifetime for these membranes cannot be provided. Nevertheless, the low elongation at break for several samples well below a 50% reduction after similar time in service indicates that the exchange interval for these membranes may need to be adjusted.

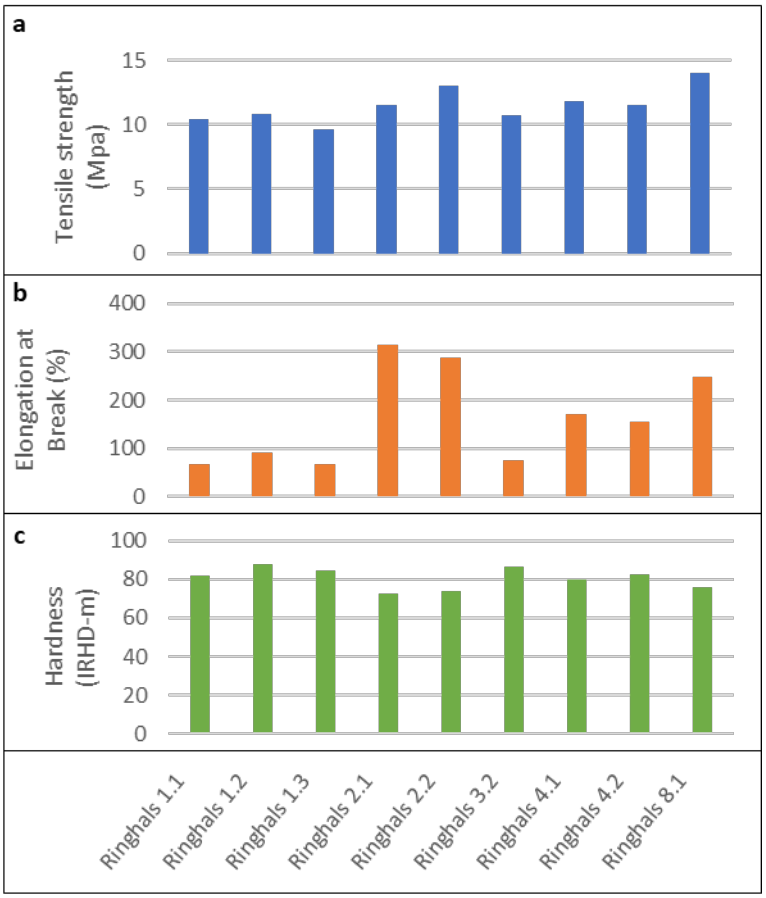

Figure 17. Tensile strength (a), elongation at break (b) and hardness (c) of neoprene membranes with a diameter of 17.5 cm as received from Ringhals NPP.

EPDM joist seal

Figure 18. Photograph of joist seal received from TVO after sample preparation.

The joist seal sample (Figure 18) has approximate dimensions of 33 × 10 cm with a thickness of 9 mm. The sample was exposed to N2- atmosphere at 45 °C during its operation at TVO for approximate 15 years. There is no relevant information regarding the initial properties of the material, such as data sheets or material specifications or pristine reference material available. Without knowing the initial material properties and the small sample amount it is very difficult to provide an analysis of the remaining lifetime of the material. Nevertheless, to gain some information on the status of the material the specimens were additionally heat-aged at 120 °C for 45 days in a ventilated oven and the tensile properties and hardness was measured.

The measurement results for both as-received and additionally heat-aged samples are listed in Table 4. The tensile strength and elongation at break did not significantly change. Instead, an increase in hardness was noted upon heat aging. The results indicate that it is possible to further age the sample, but there is no indication on its remaining lifetime possible.

Table 4. Test results for EPDM joist seals as received and heat aged for at 120°C for 45 days.

	Tensile strength (MPa)	Elongation at break (%)	Hardness (IRHD-m)
naturally aged	6,92	294,5	72,4
naturally+heat aged	7,01	283,1	78,3

CPE cables

A cable with chlorinated polyethylene (CPE) was received from Forsmark NPP (Figure 19). The cable has been removed from the NPP after about 30 years of service at a temperature slightly above room temperature and has been exposed to mineral oil fog. A cable with similar specification was purchased from Draka cables for reference.

Figure 19. Photographs of CPE cables from Forsmark NPP (left) and reference cable (right).

To estimate the total expected lifetime of the reference cables the elongation at break, the modulus at 25% elongation and the hardness of the cable jacket was measured at different intervals after aging at 90, 100, and 110°C (Figure 20). Additionally, the cable was exposed to mineral oil at 100°C to investigate a possible influence of oil exposure at the NPP. The same properties were measured for the cables received from Forsmark. For all aging temperature the elongation at break drops immediately which is more significant with increasing temperature. Instead, the modulus at 25% elongation remains nearly constant after which a sharp rise after only a few days at 110 °C was noted corresponding to a stiffening of the cable jacket. The constant plateau before the sharp increase is inversely related to the aging temperature. For both elongation at break and modulus the exposure to mineral oil at 110°C did not show any significant effect compared with aging at the same temperature without oil present. The hardness of the cable jacket with aging shows a similar trend as for the modulus with a short period of constant hardness followed by a sharp increase. The sudden onset of property changes indicate that the material is well stabilized with antioxidant to a certain point after which the oxidation of the material increases sharply.
By time-temperature superposition fitting an activation energy of 80.0 kJ/mol was estimated for aging of the CPE cable jacket. Using the master curve and an end-of-life criteria of a 50% reduction of the elongation at break yields a total expected lifetime of about 23 years. Interestingly, when comparing the cables from Forsmark which have been in service for about 30 years their properties are similar to those of the unaged reference cables. The result may either be explained by different materials in the cables from Forsmark and the reference cable, which cannot be excluded. Further studies would be necessary to confirm any difference in the materials. Or the method used may not be applicable to the type of sample. The aging mechanisms at low (service) temperatures and those at elevated aging temperatures may not be the same as is also indicated by research done within task 2.2.

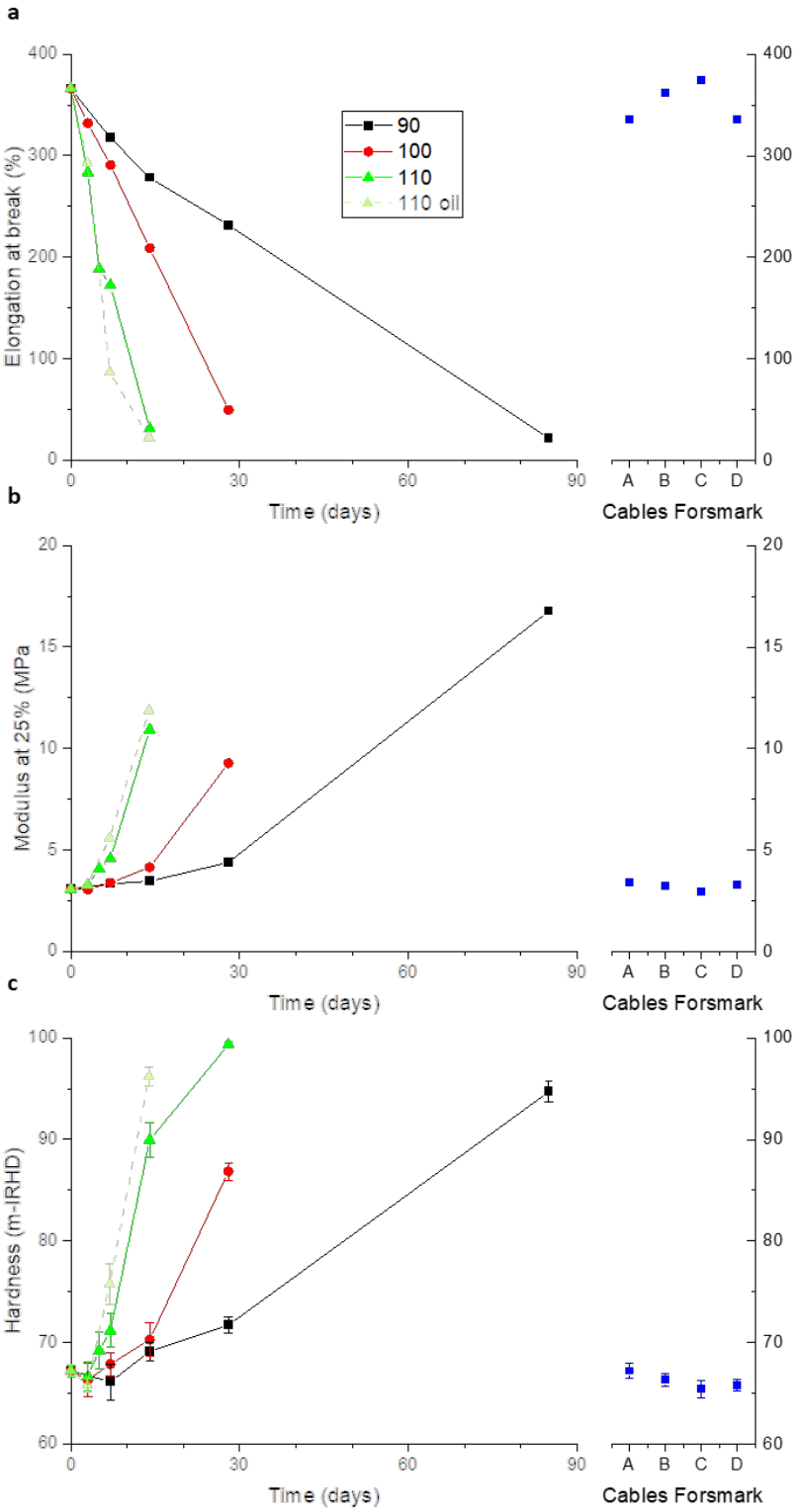

Figure 20. Elongation at break (a), Modulus at 25% elongation (b), and m-IRHD hardness (c) of CPE cable jacket aged at 90, 100, 110 °C as well as in contact with oil at 110 °C and of cables received from Ringhals. (Lines are guides to the eye.)

5.4 CONCLUSIONS

Several workshops were held, where potential material candidates from the NPPs were collected and evaluated. Materials were then chosen based on suitability and availability. The workshops were complemented by update meetings and plans to extract more samples during revisions. Unfortunately, no material could be received from Oskarshamn due to staff shortage. Test plans were set up for each material containing traditional mechanical methods to estimate lifetime and compare with materials from outtakes.

EPDM O-rings from Ringhals after their service life were tested against new reference O-rings and their total expected lifetime was determined. The O-rings were found to be of very good quality with a slow aging profile, indicating that prolonged service times may be possible after further testing.

Neoprene membranes from water pumps at Ringhals with different dimensions were investigated. For one size (19.0 cm) reference membranes were available and the total expected lifetime was estimated. Comparison of the membranes after service life with the heat aged membranes indicated that it may be possible to extend the service time of membranes.

A joint seal sample from TVO was analysed without reference by measuring tensile properties and hardness. Due to the missing reference no estimation of total or remaining lifetime was possible.

CPE cables from Forsmark were analysed and compared to a similar reference cable. A total expected lifetime of 23 years was estimated for the reference cable which is shorter than the service time of the cables from Forsmark. This may be explained by different cable jacket material or differences in the aging mechanism at low and high temperatures.

6 Online measurement to detect material degradation

6.1 BACKGROUND

Changes in the chemical structure and overall composition of the materials are likely to affect the dielectric properties and there are previous examples where changes in dielectric properties have been linked to aging of polymeric materials (Daily 2015, Li 2011, Younan et al. 1995), The effects of ageing on the dielectric behaviour of the materials in question could be measured using e.g., impedance/dielectric spectroscopy. A very convenient method to monitor the status of rubber or polymer materials would be to measure material changes online, i.e., more or less continuous measurements or non-destructive sampling of the materials as they are fulfilling their intended function. If there are large enough changes in dielectric behaviour of the materials, that can be directly related to the ageing process, it should be possible to follow these changes e.g., using resonant structures such as antenna dielectric sensors (Huang 2015, Adhikary, Biswas et al. 2017) .By broad band frequency mapping of the dielectric behaviour of the materials under test, more narrowband antenna like structures could hopefully be designed to fit the frequency providing the highest sensitivity and ease of use at lower cost. Placement, environmental factors and calibration of sensors would likely also be issues necessary to address as well as monitoring humidity and temperature to avoid overlapping effects of moisture content and degradation of the monitored polymers. This strategy towards assessment of polymer ageing has been part of Task T2.1 - Online condition monitoring techniques in the SAMPO project.

6.2 GOAL OF THE STUDY

The goal of this study was to assess if the accelerated ageing, performed within the project, induced measurable dielectric changes in some of the rubber materials and, if possible, identify specific frequency regions with more pronounced as well as systematic changes. We also wanted to investigate the feasibility of the concept of online monitoring of dielectric changes in similar rubber materials over extended periods of time.

6.3 METHODS

6.3.1 Wave guide method

As an alternative to the previously investigated dielectric probe method, it was decided to try a method for determining the dielectric properties based on placing a sample inside a waveguide and calculating the electromagnetic properties according to the Nicholson-Ross-Weir Conversion Process (Rohde & Schwarz 2012, Nicolson, Ross, 1970, Weir 1974) (see Figure 21 and Figure 22). The method was first evaluated on a lab

bench and the results can be found as a separate report ("Electromagnetic material properties of rubber blends", 2021).

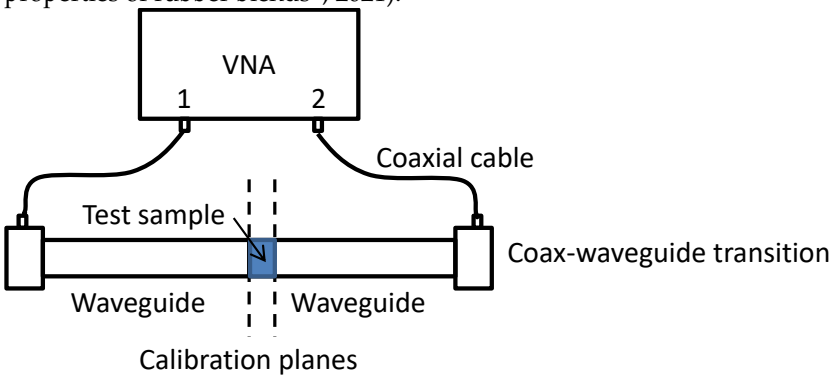

Figure 21. The waveguide setup showing the placement of the sample in the waveguide, between the calibration planes, connected to a Vector Network Analyzer (VNA) performing a two-port measurement.

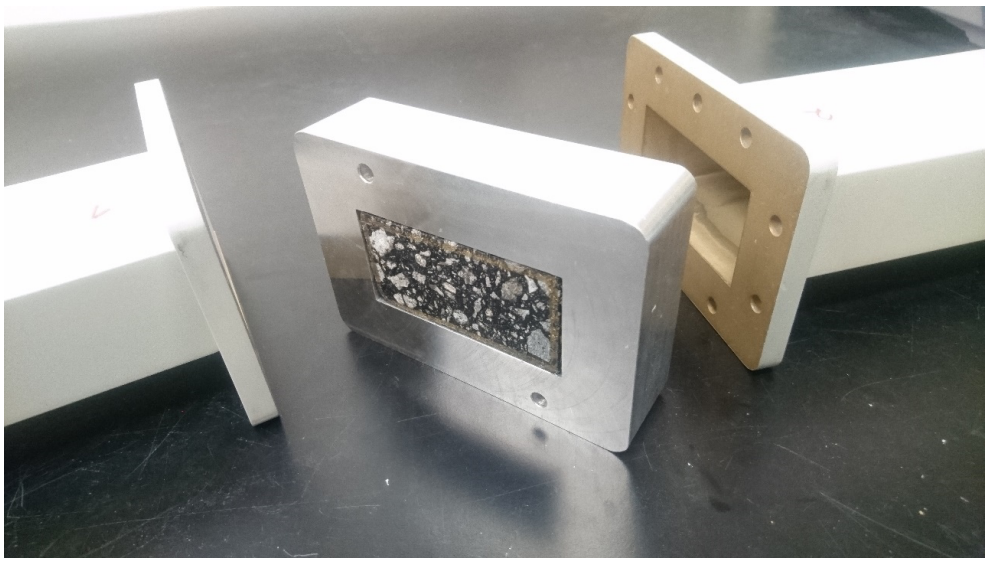

Figure 22. Waveguide with (unrelated) sample placed in sample holder. The calibration planes are adjusted in the VNA to align with the edges of the samples.

This method has less resemblance, than the dielectric probe, with the initially proposed antenna sensor but assesses the same properties. A benefit of using the waveguide measurement setup for sample material tests was that the equipment available to the project has a higher temperature tolerance, than the previously used dielectric probe, and the measurements could thus be performed at higher temperatures which should yield faster results. It should be noted that this is not something intrinsic to the specific methods, but rather to the equipment that was possible to procure for the project. The dielectric probe available had a temperature limit of 50 °C, for which we were not able to produce any clear and/or repeatable measurement results due to the very long time frame needed and the disturbance sensitivity of the method. A probe with a higher temperature tolerance might not have the same problem as ageing could be further accelerated with higher temperature.
The waveguide used will set the boundaries for the frequency space for which the method is valid and to investigate a wider range of frequencies, several different

waveguides would thus need to be used. It has previously in the project been stated that higher frequencies are of more interest as they are expected to be less sensitive to the ambient humidity. We believe this was motivated by some samples being prone to absorb some of the ambient humidity and that the dielectric constant of water is quite high at low frequencies ($\varepsilon_r \approx 80$) but rapidly decreases at higher frequencies (Barthel, Buchner, 1991) and is thus less likely to dominate the effective permittivity of e.g., polymeric materials with dielectric constants below 10. For high precision results the waveguide measurements are dependent on proper measurement of mechanical lengths related to the thickness and placement of the sample in the waveguide. This means that it will likely be more prone to errors at higher frequencies where a small error in mechanical length will be larger relative to the wavelength.

The material investigated was a commercial grade Ethylene Propylene Diene M-class rubber (EPDM, cf. grade 3, task 1.3). An image of the samples can be seen in Figure 23. The setup was first tested for stability by setting everything up in the oven, where the actual experiment was to take place, and measuring on the sample at room temperature for ~7 days.
After this, the sample was removed and the oven, with waveguide, calibration kit, and sample holder inside, was heated to the ageing temperature. Two different temperatures were used for online monitoring of the ageing polymer, 80 °C and 90 °C. When the temperature had been stabilized the setup was recalibrated.

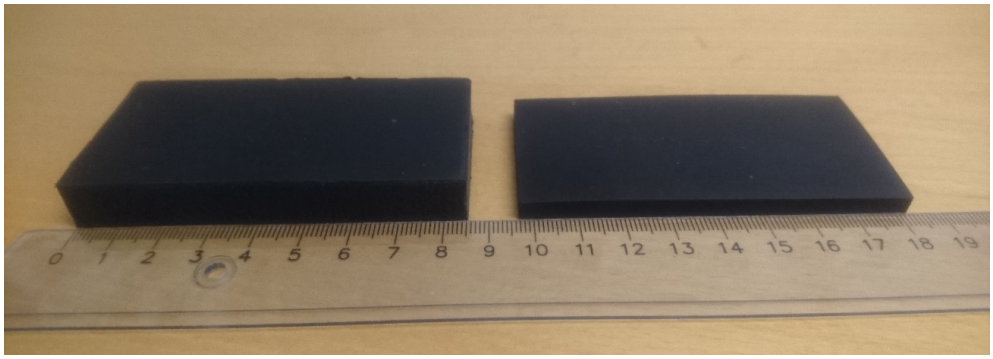

Figure 23. Rubber samples for waveguide measurements. The thicker sample, to the right, was aged at 80 °C. The thinner, to the left, was aged at 90 °C.

The room temperature sample was installed in the warm setup and measurements were started immediately. The initial heating of the sample should be taken into account when analysing the data.
The project had access to two sample pieces of suitable size and shape. The first was measured at 90 °C as this was assumed to yield fairly quick results. It was indicated in discussions with Task T2.2 that it would be preferable to perform the measurements at slightly lower temperatures as there were indications of some difference in how the samples aged. Online measurements were thus also performed at 80 °C. Unfortunately, the measurement setup was disturbed during the lower temperature measurement, and we could only retrieve reliable data for the first ~5 days of that measurement cycle. The two samples were, in these measurements, also of a different thickness. The method used should compensate for the thickness, but it may still have an impact on the results. The increased thickness will mean that the surface regions of the sample will constitute a smaller part of the entire sample. It also takes longer for the entire

sample to reach the set temperature and possibly reactive species, e.g., oxygen, would have a longer path to travel from the surface to the centre of the sample.

6.3.2 Cable measurements

The material investigated was a protective rubber insulation (chlorinated polyethylene) (CPE) around a coupled wire as that material had also been subject to mechanical testing described in section 5. It is, in fact, the mechanical breakdown that is of main interest, and changes in the electromagnetic properties would only serve as possible indicators if relatable to the mechanical changes.

Cross talk measurements

Since little was known about the use of the cables, it was decided to try to use some generalized method of measurement related to the cable impedance. Initially, a method used for investigating shielded cables, by inspecting cross-talk, was tried.

In the original setup the investigated cables were, in a parallel pair, suspended at a constant distance over a ground plane, and each cable is in one end connected to a vector network analyser (VNA), and in the other end terminated with a 50 Ω load. If the VNA is connected to the cables in the same end it is called Near End Cross Talk (NEXT), and in the opposite ends it is called Far End Cross Talk (FEXT). Our hope was that changes in the cable insulation could be traced to the scattering parameters for the different cases, of the system.

The 50 Ω load terminations were chosen as it was assumed that would be closest to something that would be found in a real installation, and to have the same load at both ends of the cables (the port impedance of the VNA is 50 Ω). To achieve a more distinct reflection it was also tested to instead measure with the end of the cables shorted.

Cables were cut to 0.5 m and the conductor wire pair of each cable, were both soldered to N-contacts in both ends. These were in turn attached to two copper angle brackets attached to a large copper ground plane. The angle brackets were located opposite each other and adjusted so that the cables were in a stretched state between them, to ensure that the distance from the ground plane along the cables would be as constant as possible. The distance from the centre of the cable attachment points to the ground plane was 3.3 cm. There were very few samples available for measurement, likely because the cables were not initially intended for this type of measurement but were rather left over from the mechanical testing (see section 5). With this setup we ended up measuring only one aged cable and two unaged cables. The different combinations of these cables were all investigated. To somewhat minimize the influence of mounting the cables differently, or rather to introduce a new error for each individual measurement, we removed the cables and remounted them in a new position between different measurements as well as measurement types.

Figure 24. Cables mounted and taped to run parallel above the ground plane. The connectors are located on the outside of the copper angle brackets. Each of the wires is connected to the VNA in one end and a termination (50 Ω or short) is connected to the other end of that wire. If the wires are connected to the VNA at the same end, we call the measurement NEXT. If they are connected at opposite ends, we call it FEXT.

Reflectometry

To isolate the effect on each cable sample, they were also measured with only one cable mounted at a time. In this case we shorted the cable in the far end to achieve a well-defined reflection.

Parallel plate impedance measurements

Some initial low frequency impedance measurements were performed on neoprene rubber samples cut from membranes (cf. task 1.1).
The rubber sample is sandwiched between two copper electrodes to create a structure similar to a parallel plate capacitor. The materials were characterized over the interval 0.1 Hz – 20 MHz. Unaged samples were characterized as well as samples aged at 90 or 100 °C for two weeks. The impedance is normalized by the overlapping area of the electrodes and the thickness of the samples.

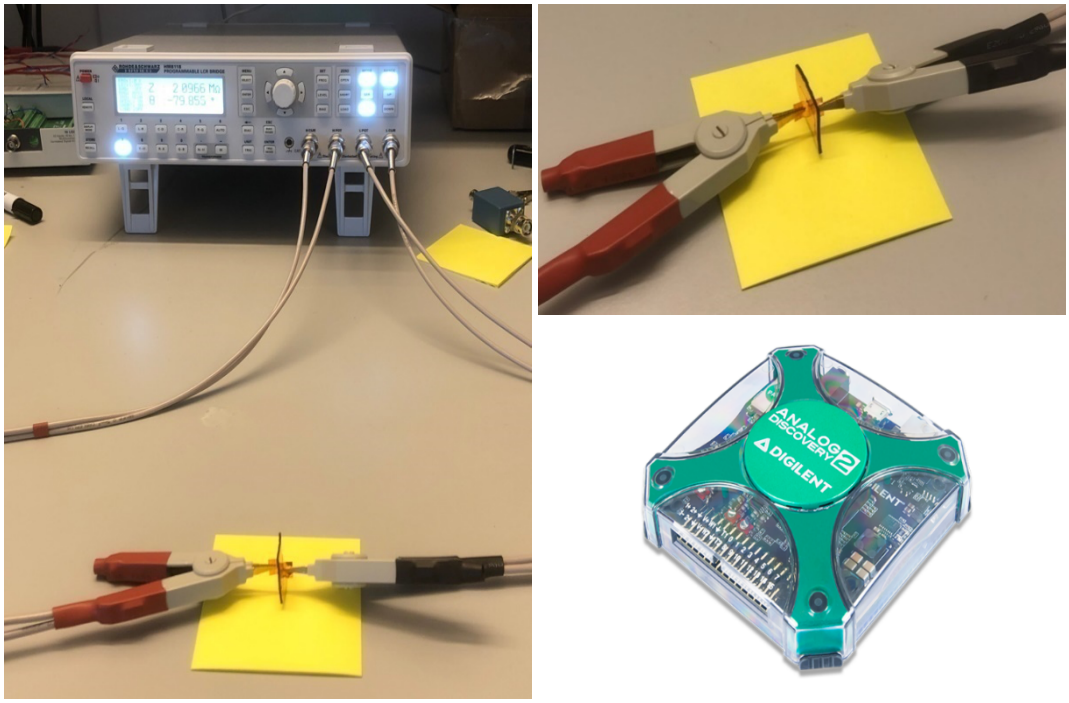

Figure 25. (Left) LCR Hameg HM8118 Rohde & Schwarz was used to measure impedance in the frequency range of 20 Hz to 100 kHz, (Right top) sample configuration (plate capacitance) with electrodes between the sample, (Right bottom) Analog discovery 2 that was used for impedance measurements between 0.1 Hz and 20 MHz.

6.4 RESULTS AND DISCUSSION

6.4.1 Wave guide method

The stability check of the measurement set-up showed that there was some drift in the results and revealed some form of periodic low frequency background signal which is estimated to possibly introduce an error of <~0.4% on the calculated permittivity value of the specific material under test. Even though the noise could be considered low, a simple low pass (Moving Average) filter, corresponding to approximately 50 minutes, was applied to filter remove the background noise.

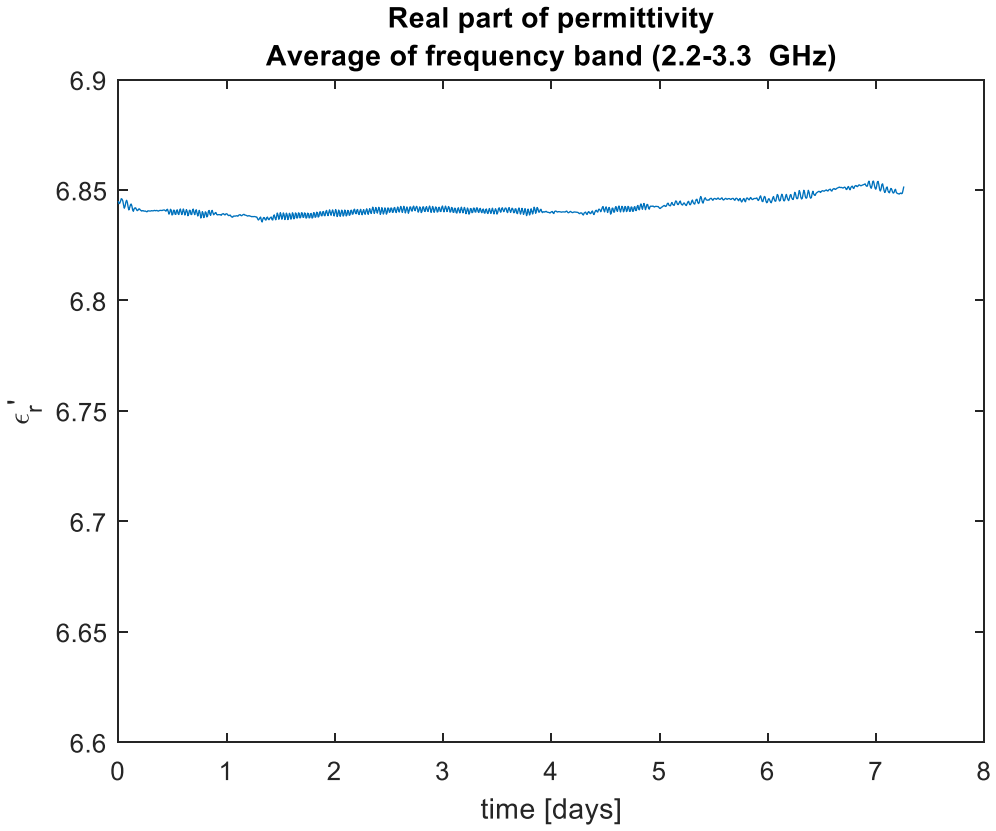

Figure 26. EPDM real part of relative permittivity at room temperature. Online measurement over one week.

The stability of the method and the material over one week at room temperature can be seen in Figure 26. EPDM real part of relative permittivity at room temperature. Online measurement over one week.

For the online measurements at the more elevated temperature (90 °C), changes to the material properties appear to start immediately (see Figure 27). The early changes in permittivity are also more dramatic and properties appear to level off after a little more than a week and an apparent change of ~3 % in permittivity from $\varepsilon_r \approx 6.8$ to $\varepsilon_r \approx 6.6$.

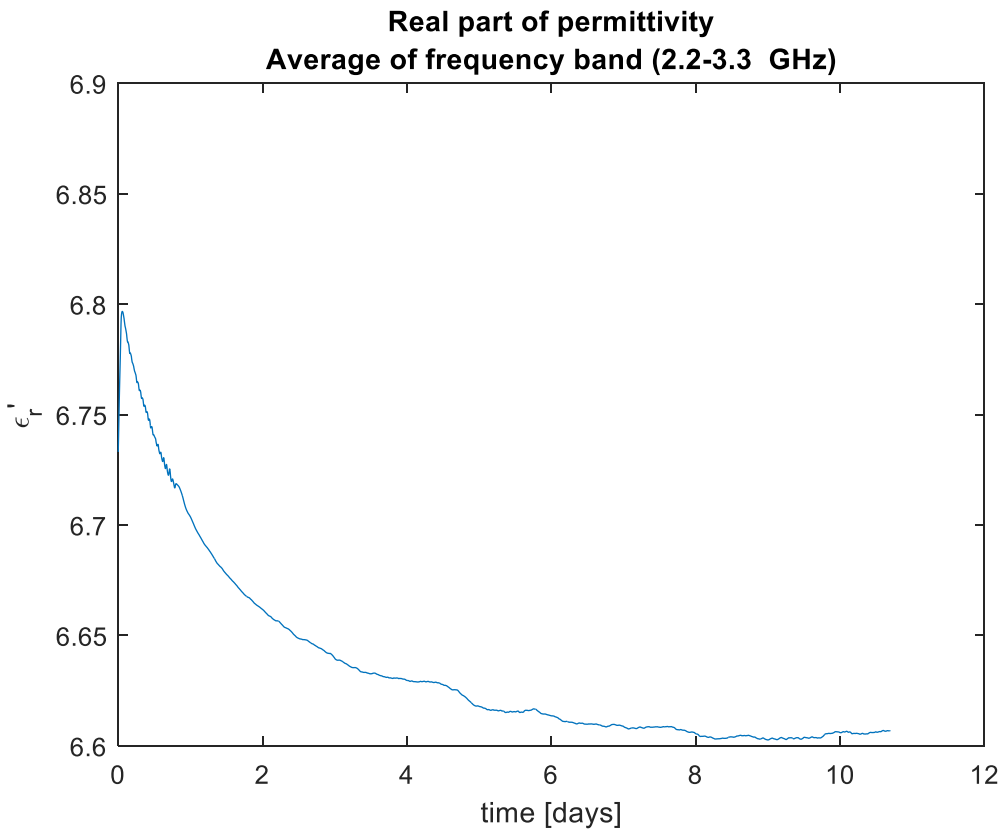

Figure 27. EPDM real part of relative permittivity at 90 °C. Online measurements

There were some differences observed for the measurements at 80°C (Figure 28) as compared to those at 90°C. First, the initial increase in permittivity that can be seen for both temperatures is noticeably slower for the lower temperatures. This could likely be explained by the sample, used for the 80°C measurement, being of about twice the thickness, thus taking longer for the entire sample to get warm. Second, the initial permittivity appears much lower, even from the very start. It is difficult to speculate as to why this is, but the fit of this sample to the sample holder was not as good and it is possible that there could have been a small misplacement in the sample holder or small air gaps along one or more of the sample edges leading to this error. We still believe the overall behaviour could be used as an indicator of how the samples would change with ageing. After the initial increase of permittivity, it starts to fall off also for this temperature, but at a much slower rate. It would have been interesting to see if this trend would continue and could be compared to the measurements at higher temperatures, but this was not possible due to lack of test materials as well as the equipment not being possible to book for these prolonged times.

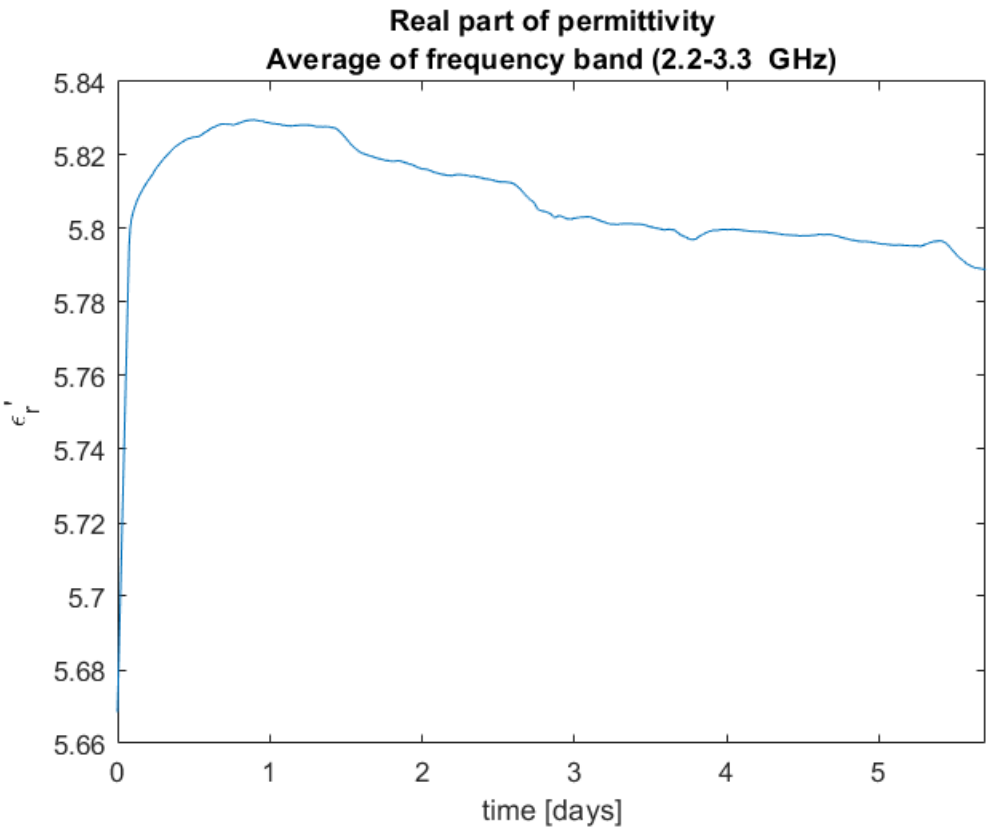

Figure 28. EPDM real part of relative permittivity at 80 °C. Online measurements

6.4.2 Cable measurements

Several measurements of the same type have been performed. In the figures of this section, it is the (linear) mean of the measurements of the same type that are presented as representations of that measurement type.

Cross talk measurements

Two-cable S-parameter measurement results can be seen in Figure 29-Figure 34. When the aged cable is included in the measurements, it is attached to port 2 of the VNA. When inspecting the frequency response from the measurements where the cables are terminated with a 50 Ω load (Figure 29-Figure 31), there is only a very small difference in location of frequency dips of S11 as well as S22, even though they are measuring the response on the two different cables in the measurement. Upon first inspection, the first clearly pronounced dip can be found around 270 MHz. This corresponds to a wavelength in air of about 1.1 m, which coincides quite well with twice the cable length (2*0.5 m). This would mean that the effective permittivity is only slightly higher than that of air. The difference in mean location (frequency) between the Aged-Unaged (A-U) cable pair as compared to the Unaged-Unaged (U-U) pair is around 1% for both S11 and S22 both when looking at NEXT as well as FEXT. This would correspond to a change in dielectric constant of about 2%. This change is too small to determine if it is significant without performing more measurements. It is interesting to note that the reflection coefficient changes in a similar manner on both ports (S11, S22), even though it is only the cable on port 2 that is changed to an aged cable. Upon closer inspection,

there does appear to be the tendency of a smaller dip in S11 and S22 a slightly lower frequency and yet again at what could be twice that lower frequency. At these, less pronounced dips, the frequency shift between the U-U and A-U measurements appears to be larger and in the opposite direction from what was observed for the 270 MHz dip.

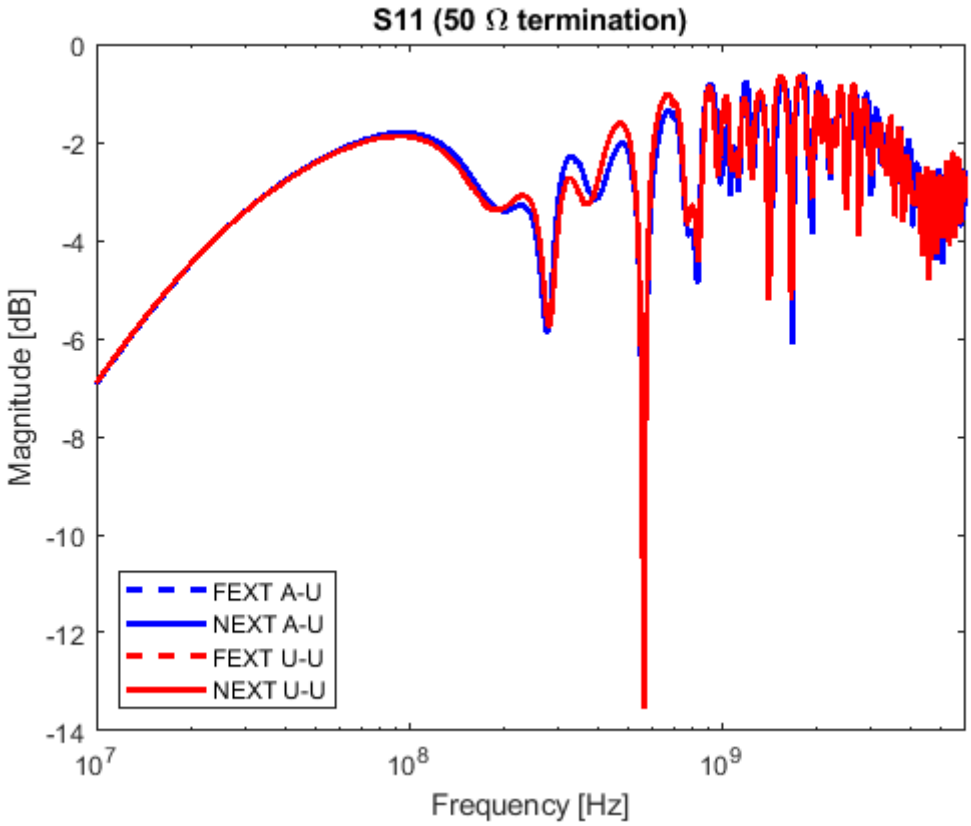

Figure 29. Far End Cross Talk (FEXT) and Near End Cross Talk (NEXT) S11 of a system of two parallel cables above ground plane where the end of each cable is terminated with a 50 Ω load. Line colours indicate the type pairing of the two wires. Blue – one aged and one unaged cable. Red – two unaged cables. Aged cable is connected to port 2.

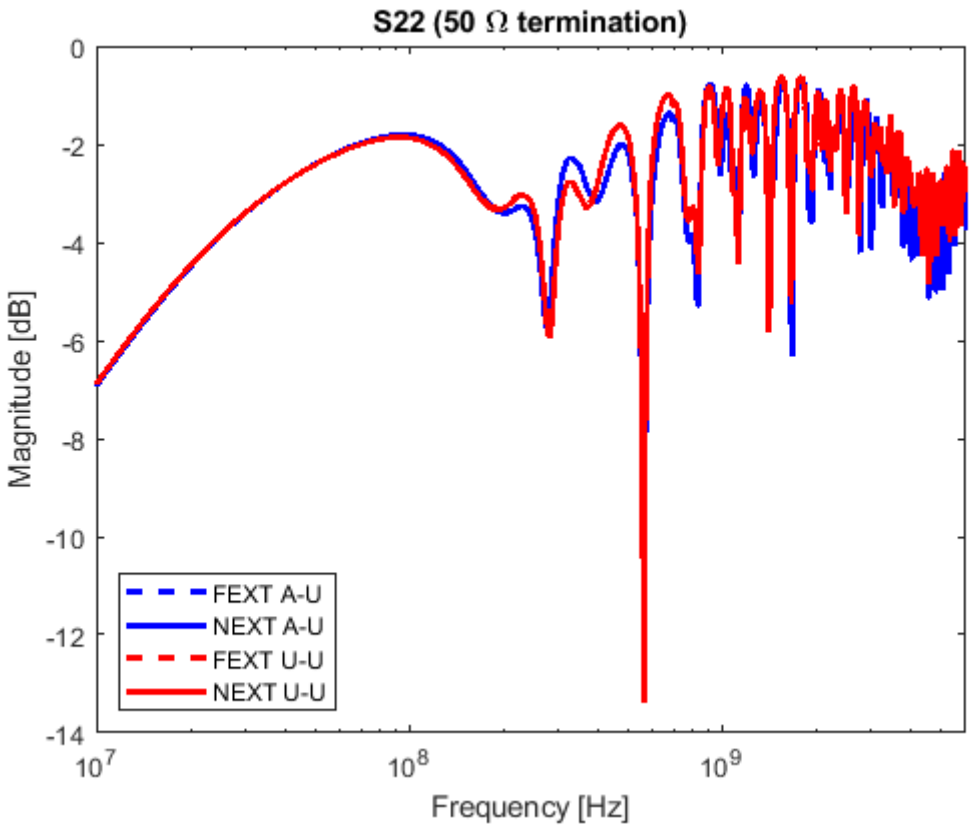

Figure 30. Far End Cross Talk (FEXT) and Near End Cross Talk (NEXT) S22 of a system of two parallel cables above ground plane where the end of each cable is terminated with a 50 Ω load. Line colours indicate the type pairing of the two wires. Blue – one aged and one unaged cable. Red – two unaged cables. Aged cable is connected to port 2.

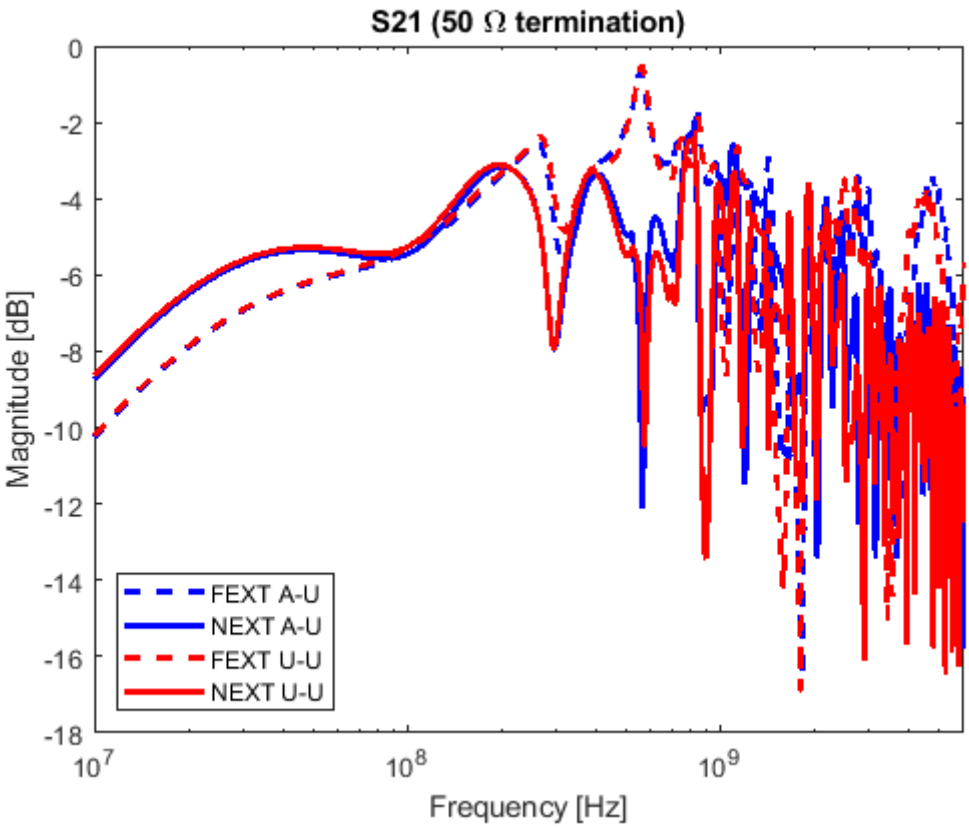

Figure 31. Far End Cross Talk (FEXT) and Near End Cross Talk (NEXT) S21 of a system of two parallel cables above ground plane where the end of each cable is terminated with a 50 Ω load. Line colours indicate the type pairing of the two wires. Blue – one aged and one unaged cable. Red – two unaged cables.

When the cable ends are shorted (Figure 32-Figure 34), the dips at lower frequencies emerges more clearly and the frequency is identified as of around 185 MHz. If this dip is due to a cable resonance it would correspond to an electrical length of about 0.8 m, which is much longer than the cable length of 0.5 m. If assuming this is indeed a resonance from the length of the cable, the effective relative permittivity can be calculated from this relation and would then appear to be around $\varepsilon_r \approx 2.5$ at this frequency.

The shift in frequency for the 185 MHz dip, when exchanging one unaged cable to an aged one, is more than 3%, which would correspond to a ~6.5 % change in ε_r. It would be expected to find another dip at the next resonance, which should be possible to find at about twice the frequency of the first frequency dip. There is indeed a dip close to 380 MHz. The shift in frequency at this dip is even more pronounced and would correspond to a change in epsilon of almost 10 %. Looking for the further resonances proved more difficult as the data becomes a little noisier, but it was possible to identify dips at ~560 MHz with a similar shift between the aged and the unaged cables.

It should again be noted that the shift of the 185 MHz dip and the 270 MHz dip are in opposite directions. We are yet to find any good explanation for this.

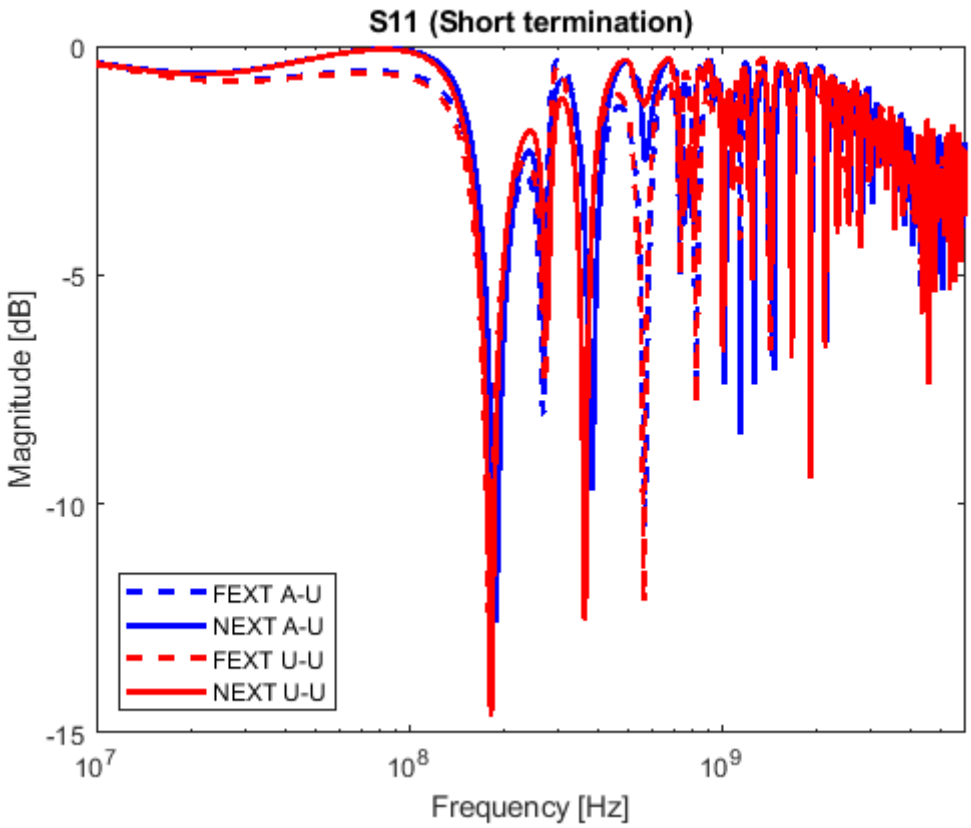

Figure 32. Far End Cross Talk (FEXT) and Near End Cross Talk (NEXT) S11 of a system of two parallel cables above ground plane where the end of each cable is terminated with a connection to ground (short). Line colours indicate the type pairing of the two wires. Blue – one aged and one unaged cable. Red – two unaged cables. Aged cable is connected to port 2.

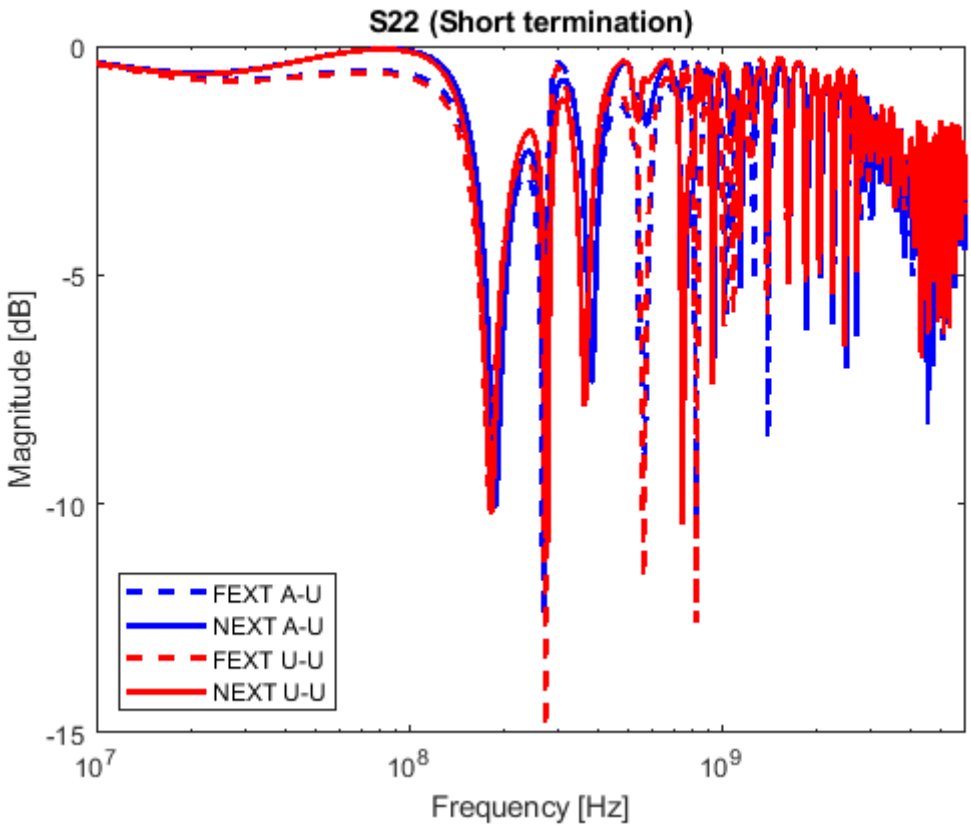

Figure 33. Far End Cross Talk (FEXT) and Near End Cross Talk (NEXT) S22 of a system of two parallel cables above ground plane where the end of each cable is terminated with a connection to ground (short). Line colours indicate the type pairing of the two wires. Blue – one aged and one unaged cable. Red – two unaged cables. Aged cable is connected to port 2.

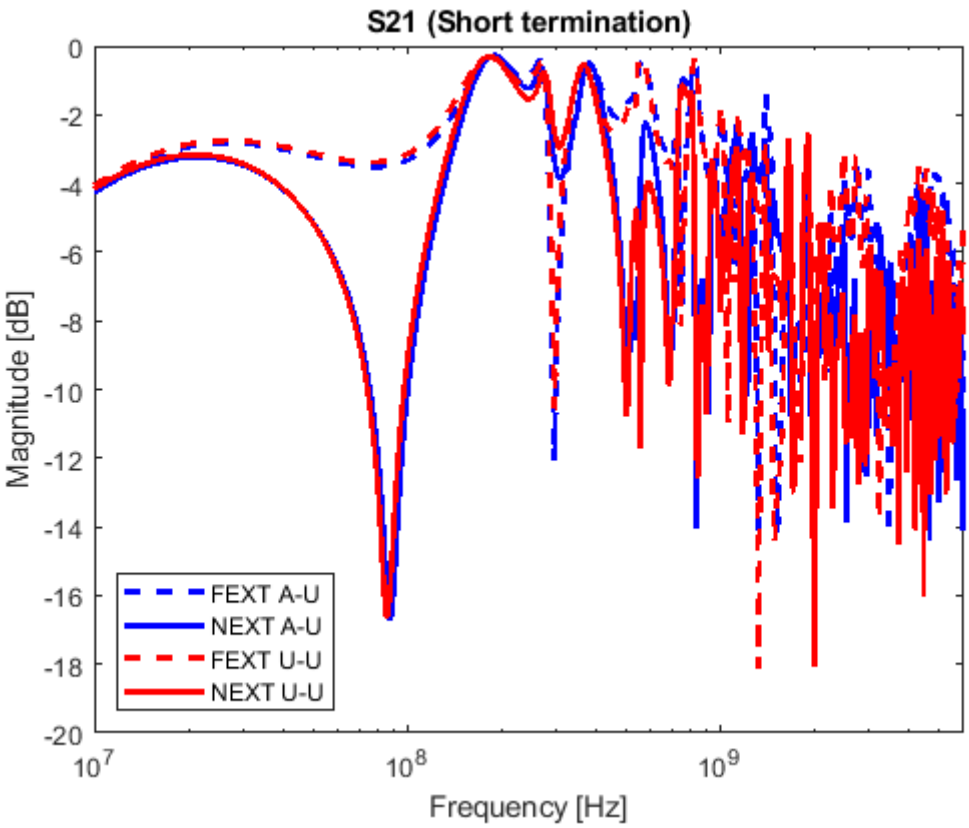

Figure 34. Far End Cross Talk (FEXT) and Near End Cross Talk (NEXT) S21 of a system of two parallel cables above ground plane where the end of each cable is terminated with a connection to ground (short). Line colours indicate the type pairing of the two wires. Blue – one aged and one unaged cable. Red – two unaged cables.

Reflectometry

When looking at the S11-data (Figure 35) from the cables mounted one at a time, the difference between the aged and the unaged cables appears almost non-existant. The the lowest frequency with an identifiable dip at is here clearly found around 270 MHz. The frequency shift of the dips in S11 is at most found to be less than 0.5 % which is probably too small to consider significant eventhough the direction of the shift is consistant with what was observed for the cross talk measurements at the 270 MHz dip.

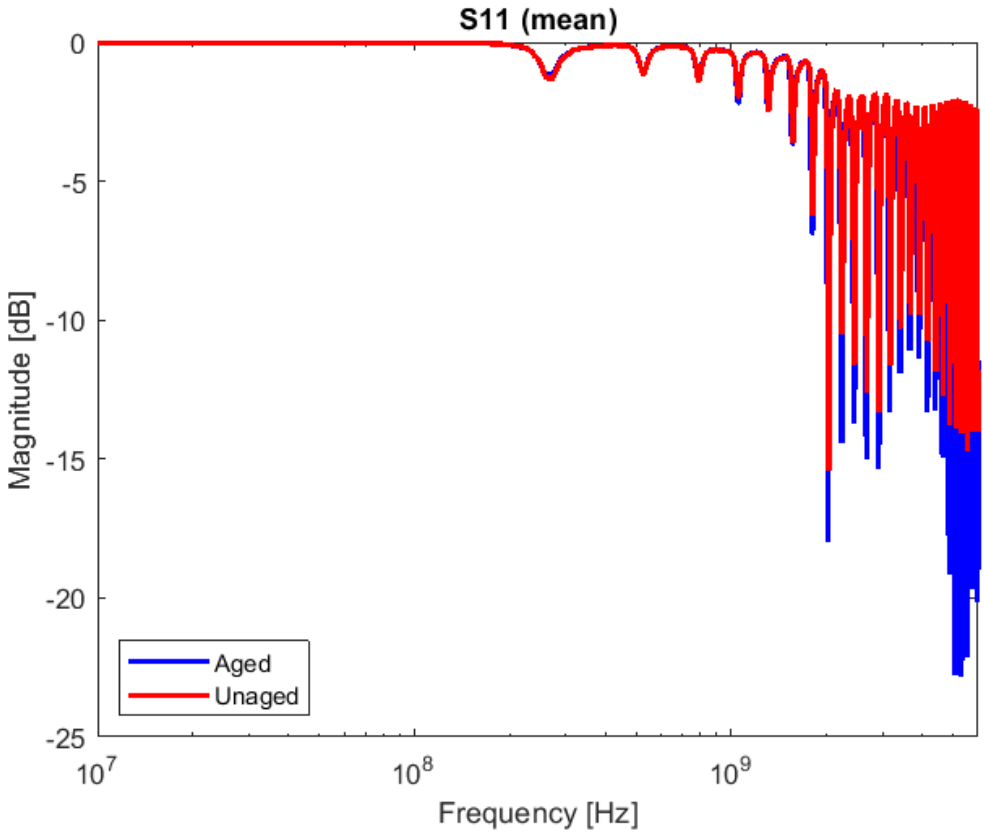

Figure 35. S11 of single cables above ground plane where the end of the cable is terminated with a connection to ground (short). Line colours indicate the type of wire. Blue – aged cable. Red – unaged cable.

It is possible to try to compare the elctrical length of the cables by transforming the data from frequency domain to time domain (Figure 36-Figure 39). The frequency sampling was in some cases logarithmically spaced and a non-uniform inverse DFT had to be used, which could introduce some artifacts (e.g. ringing). The time data was scaled by the speed of light to instead show electrical distance travelled along the cable. As S11 (and S22) is the reflected signal at each port, the distance is here also divided by two to compensate for the signal travelling to and from the reflection point. There is an initial large reflection due to impedance mismatch at the very contact point closest to the VNA. The main reflection then shows up at a distance of a little more than 0.5 m, as the electrical length of the cable is slightly more than the mechanical length (signal velocity is slower than the speed of light). Similar reflection patterns can be seen reoccuring with decreasing signal strength at n-times the distance to the main reflection as the signal travels back and forth along the cable. The reflection appears somewhat indistinct, which could be due to the state of the cable close to the contacts where it has been stripped and soldered. This may add to the explanation why the data becomes a little more chaotic at higher frequencies

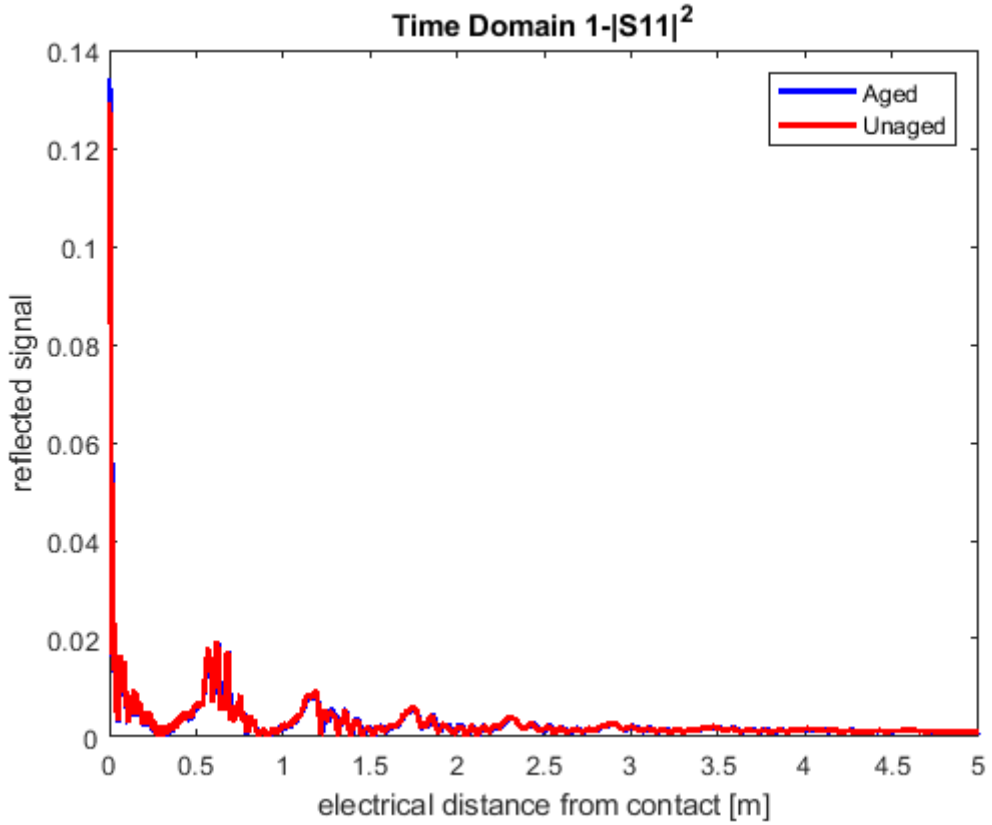

Figure 36. Reflected signal from along the wire calculated from S11 frequency data. The underlying frequency data is logarithmically spaced which could explain some of the spread of the peaks and/or apparent ringing behaviour of the signal. For both aged (blue) and unaged (red) cables the reflection at the far end of the cable appears to occur at an electrical distance of ~0.6 m.

The single cable time domain measurements were repeated with lineary spaced frequency samples showing that the reflection in reality probably is a little bit sharper. The amplitude appears slightly lower for the aged cables, but that could probably be attributed to a differences in the contacts. As S11 is a relation between the incident and reflected power waves it can never add up to more than 1 and the amplitudes of peaks further down the cable will thus be affected by a stronger initial reflection.

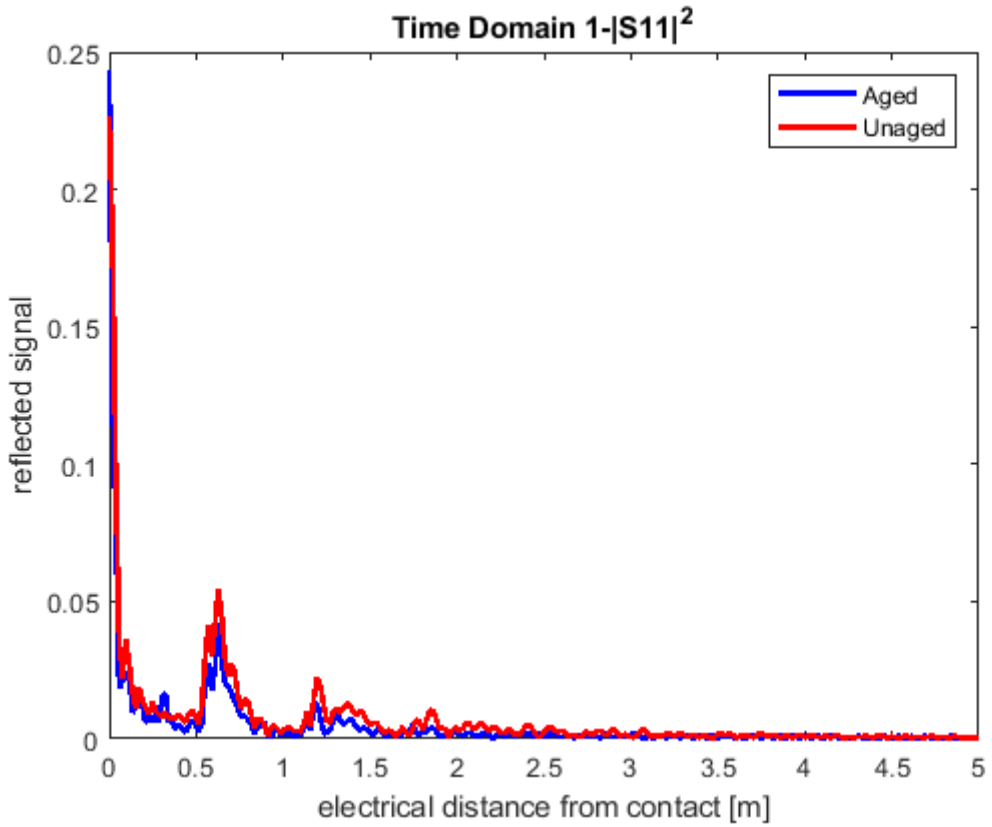

Figure 37. Reflected energy along single cables calculated from linearly spaced frequency data. The initial contact show a quite large reflection, but the first reflection further in on the cables is at ~0.6 m. The difference in amplitude between the curves is likely due to the first reflection being larger for the aged sample. This is likely an effect of the contact rather than the sample.

It is also possible to transform the reflected signal of the cross-talk measurements to try to locate the reflections (Figure 38-Figure 39). The frequency samples in these measurements were all log-spaced which could introduce artefacts and one should be careful drawing conclusions. This was unfortunately realized too late and more time would be needed to repeat the experiment with more carefully chosen measurement parameters.

For the dual cable measurements there appears to be more reflections possible along the entire length of the cable. By this, we are referring to the more spread out initial values from ~0-0.4 m. This effect is more pronounced for the FEXT-measurements. The largest reflection (after the first contact reflection) is indeed located at ~0.8 m, but there appears to be another small peak, approximately at the same location as where it was found for the single cable measurements (~0.5-0.6 m)

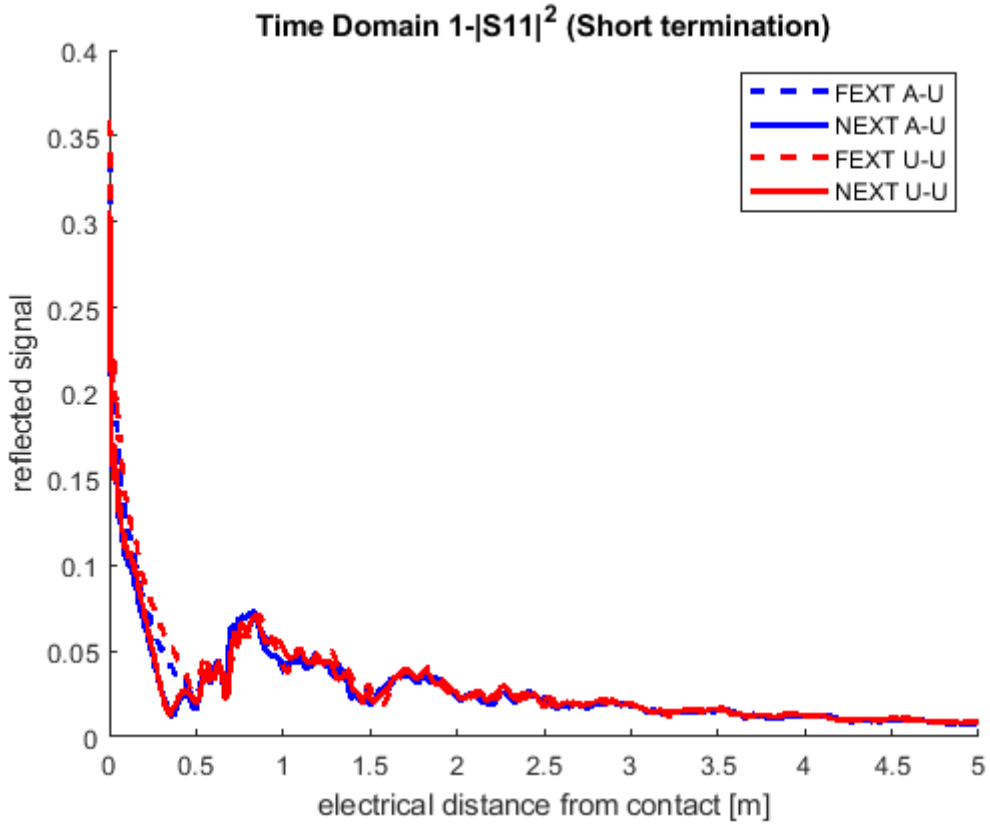

Figure 38. Reflected energy along the cable length with a second cable attached in contact. The measurements are named by the measurement type (FEXT/NEXT) and cables involved (Aged-Unaged/Unaged-Unaged). The entire lenght of the cable appear to show some reflected energy, but peaks can be seen at ~0.6 m and ~0.8 m

With the 50 Ω load (Figure 39) it is much more difficult so see something in the data in this form. This should not be surprising as it would be expected to have fewer sharp transitions in impedance. There are however two noticable peaks. The first, again at ~0.5-0.6 m, and then another one at a little more than ~0.7 m. Again there is no large difference between tha aged and unaged cables for the first peak while the second one moves in the same manner as was observed for the second peak in the measurements with the shorted ends (Figure 38). The shift is however slightly smaller than what was estimated looking at the frequency data. It is a lot more difficult to identify peak values of these reflections in the time domain as compared to some of the dips in the frequency domain.

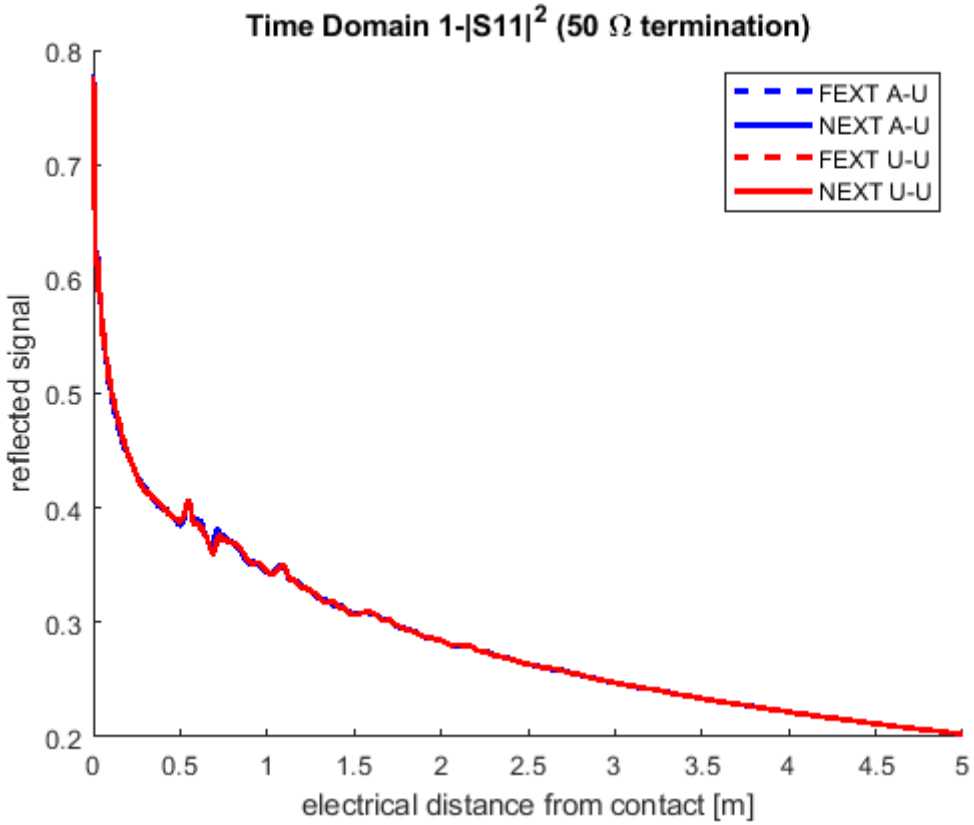

Figure 39. Reflected energy along the cable length with a second cable attached in contact. The measurements are named by the measurement type (FEXT/NEXT) and cables involved (Aged-Unaged/Unaged-Unaged). The entire lenght of the cable show reflected energy, but small peaks can be noticed at ~0.6 m and ~0.8 m

6.4.3 Parallel plate impedance measurements

The results of sample ageing regarding the electrical impedance measurements are most clear at very low frequencies where the impedance appear to increase with increased ageing of the samples (2 weeks at 90°C and 100°C as indicated in Figure 40 compared to new rubber material). The phase angle also goes down at low frequencies indicating that the aged samples here show a more capacitive behaviour, while the pristine samples show a slightly more resistive behaviour. It cannot, at this time, be stated that this should be a general expectation without knowing the responsible ageing mechanism. These preliminary results non the less clearly show an effect of the aging on the impedance and thus renders the technique an attractive candidate for further investigation.

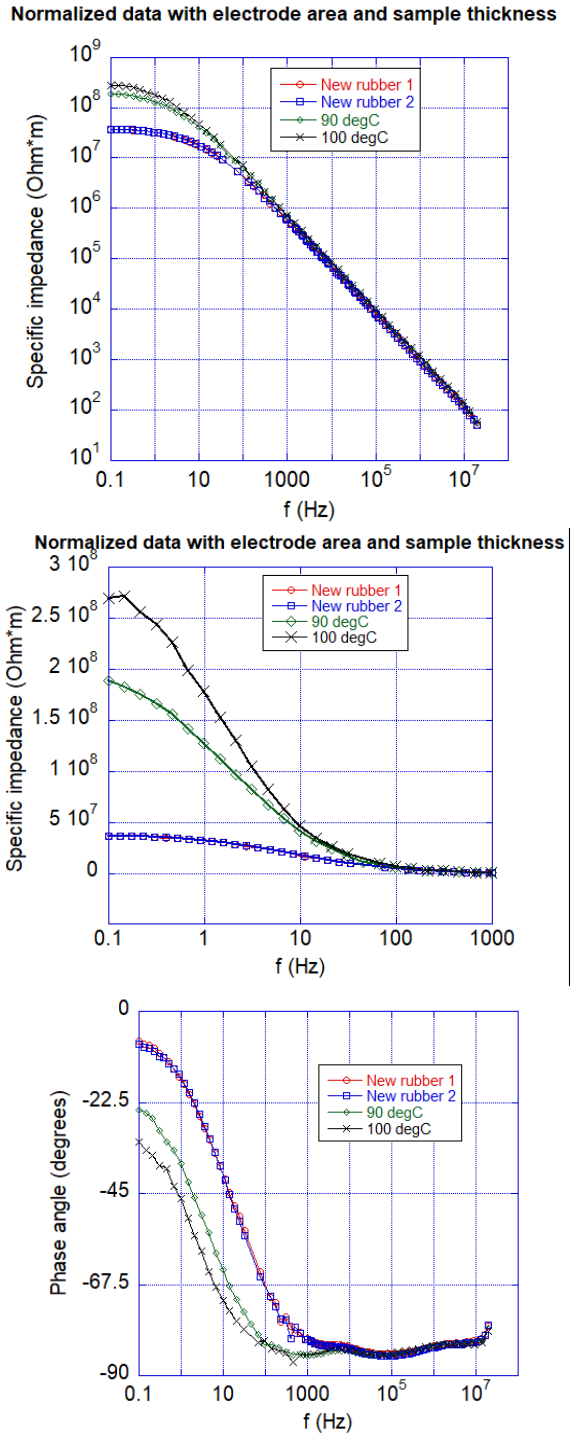

Figure 40. (top) Specific impedance (normalized with electrode area and sample thickness), (middle) zoomed in specific impedance at frequencies below 1 kHz and (bottom) phase angle (between excitation voltage and current), and versus excitation frequency. New rubber 1 and 2 are two fresh rubber samples and 90 degC and 100 degC are aged rubber samples aged in an oven for 2 weeks at 90 °C and 100 °C.

6.5 CONCLUSIONS

6.5.1 Waveguide method

Measurement results achieved can be seen as indications that the permittivity might yet prove a useful indicator for aging monitoring of some polymeric materials. The reason for the seen reduction in permittivity is yet to be investigated. It should thus not be expected that all materials would behave the same. If the change in permittivity is due to the consumption of some component, the trend might also change at later stages of ageing of the material. If the changes can be tied to some specific reaction, the method could thus prove to be very useful for understanding approximately where in the ageing process a well-known material could be. A weakness of the method would be that the entire course of ageing would likely need to be recorded for the method to be of much use. The changes here recorded are also fairly small. It remains to see if the changes are still large enough to use a passive structure, like a simple resonance circuit or antenna-like element, as a probe.

6.5.2 Cable measurements

Inspecting a single cable as it was done here appears to have provided very little information. We have come to realize that this might be due to poor experimental design. As the distance from the cable to ground is much larger than the thickness of the cable the effective permittivity will likely be dominated by the air between the cable and the ground plane. It would probably be a good idea for future measurements to place the cables directly on the ground plane or to create a coaxial structure with ground surrounding the insulating material.

When two cables were connected, we could however see some effect. This is probably because they are in much closer proximity and the effective permittivity between the cables is thus dominated by the CPE insulator instead of air. Even if only one cable was exchanged, from an unaged cable to an aged one, the effect could be observed in the reflection of both cables. We would suggest that this, together with the fact that it is more pronounced for the setup with shorted ends, shows that at least a part of the return current happens in the coupled conductor. If cables are mounted in a bundle, it could thus likely be useful to investigate them at least pairwise so that the effective permittivity of the cable will be dominated by the insulation material between the cables, and any distance to some other ground plane will be of less significance. In our measurements only one of the cables have been aged. If our argumentation is correct, the effective permittivity of the coupled cables should be dependent on the insulation material around both cables. If the other cable is aged as well, a larger effect on the effective permittivity should thus be expected.

The analysis could likely be improved by more in-depth circuit models to further understand the relation between the material changes and the effect on the measurements. This would likely also help in improving the measurement set-up. Unfortunately, there has not been time for this type of analysis as the samples arrived quite late in the project. The number of available samples have unfortunately not been large enough to properly evaluate the method with valid uncertainty estimates. This would have to be changed if the work is to be continued.

The method could likely be adapted to an online measurement set-up with the cables under test located in a hot/warm environment.

6.5.3 Parallel plate impedance measurements

Even though there have previously been expressed concern towards working at low frequencies due to the, sometimes, humid environment and the effect the wet atmosphere might have on the measurements, the results from these measurements show a clearly visible effect of the ageing. This renders them interesting for further investigation. One way forward would be to try to construct equivalent circuits with elements related to the different ageing mechanisms.

7 More sensitive analysing techniques

7.1 GOAL OF THE STUDY

The goal of this study was to investigate, if microcalorimeter can be used as a complementary technique to the widely accepted ATA (Accelerated Thermal Ageing), to predict service lifetime of polymer materials. To be able to measure changes in the material properties before and after accelerated thermal ageing rather high exposure temperatures are necessary. Therefore, microcalorimetry in which thermal degradation can be studied closer to the real-life temperatures would be a valuable tool, provided that microcalorimeter data can be used for the determination of activation energies.

7.2 METHODS

Microcalorimetry (MC) is one of the most sensitive calorimeter techniques, and significantly more sensitive than differential scanning calorimeters (DSC). Both types of instruments can measure a signal in the order of μW, however, the sample mass in isothermal microcalorimetry (IMC) can be in grams (1-10 g), whereas DSC uses milligram sample mass. Therefore, the specific sensitivity in μW/g for IMC can roughly be at least 1000 times higher than for DSC. This also means that endothermic or exothermic processes due to chemical and/or biological and/or physical changes, can be studied at 100 °C lower than the DSC. For example, instead of accelerated thermal ageing at 150 °C, thermal degradation using TAM can be studied at 50 °C, which is much closer to the real-life operating temperatures.

Lifetime predictions are based on the fact that all chemical reactions proceed faster at a higher temperature. However, the Arrhenius equation is valid for low molecular substances and not polymers. There are important assumptions associated with using Arrhenius relationship for polymers, for example a single degradation mechanism valid for higher as well as lower temperatures and reaction parameters remain constant. Arrhenius plot using different parameters for instance ageing time, reaction rates (k) or degradation times ($1/k$), vs $1/T$ (ageing temperature in Kelvin) allow life-time prediction using data obtained at elevated temperatures (ATA) and can be extrapolated to real-life temperatures. In ATA, which is one of the widely accepted technique thermal ageing is performed at elevated temperatures as aforesaid and life of the material closer to the real-life operating temperatures is then calculated by extrapolation. It involves the use of Arrhenius equation which, states that lifetimes are proportional to exp ($-E/RT$), here E is the activation energy for the chemical process responsible for the degradation of polymeric material. Several studies have shown that extrapolation is sensitive to the reaction parameters for example activation energy (E). Because E is determined at elevated temperatures and may not be valid at lower temperatures. For EPDM Arrhenius plot over a wide range of temperature 50-170 °C, has shown a curvature and significant difference in the activation energies obtained using higher temperatures ($E \approx 115$ KJ/mol) and lower temperatures ($E \approx 75$ KJ/mol) (Celina, Gillen et al. 2005 and Forsström, Svensson et al. 2000).

7.2.1 Materials and Microcalorimeter tests

An experiment was conducted using a sample known as Tremco sealing. The joint was Tremco Proseal or Tremco Dymeric. The Tremco sealing was used in the OKG NPP for about 30 years. It was not possible to get a fresh sealing material so that comparative study can be conducted between same materials.
For comparison the Tremco sealing and grade 1 or model material was also tested in MC. The detailed information/recipe of the model material is specified in an article by Mohit pushp and cowerkers (Pushp, Lönnermark et al. 2023).

MC was operated at 90 °C. A reason for the selection of temperature was to compare the behaviour of both materials and to observe what can be learned for the MC test. A quasi-isothermal test using only Tremco sealing was also conducted 60-100 °C.

Information about Tremco sealing obtained from NPP. Figure 41 and Figure 42, show the location of Tremco sealing.

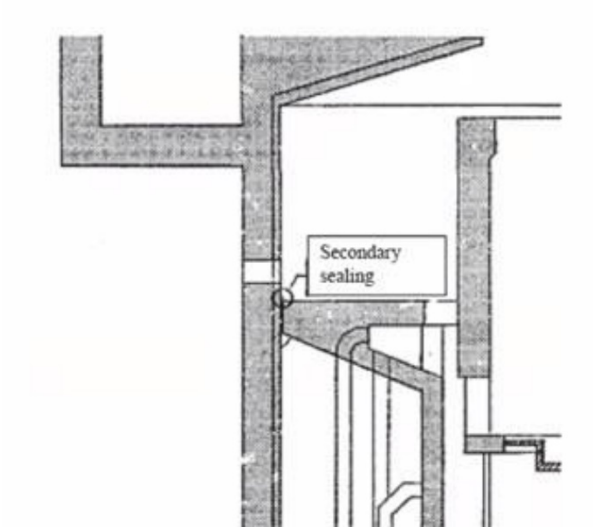

Figure 41. Tremco sealing location used in NPP

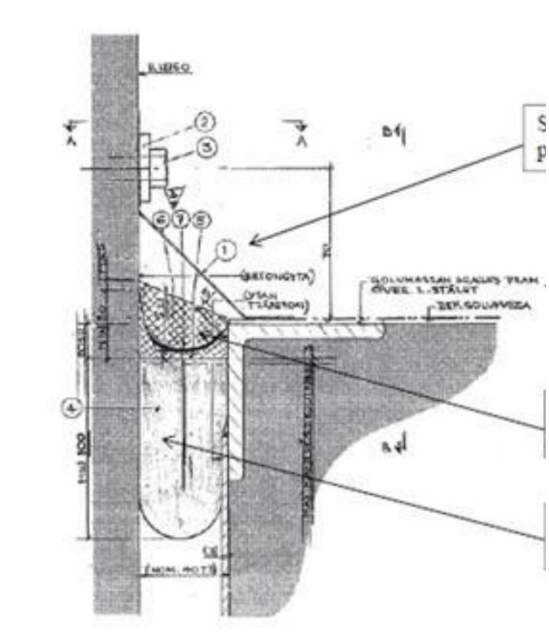

Figure 42. Tremco sealing location used in NPP

7.2.2 Technical parameters of TAMIII.

Temperature accuracy,
A temperature or baseline stability or drift of the heat flow signal is utterly important. If the heat flow signal drifts higher than baseline, then it may be interpreted as the exothermic processes and endothermic for heat flow signal lower than the baseline. The heat flow and heat for one of the microcalorimeters installed in TAM III were measured for about three weeks as shown in Figure 43. The heat flow stability was ± 0.1 µW and the negligible heat was obtained after integrating heat flow over time. This indicates that the heat flow for example 1 µW which was measured using EPDM samples was due to chemical changes in the material.

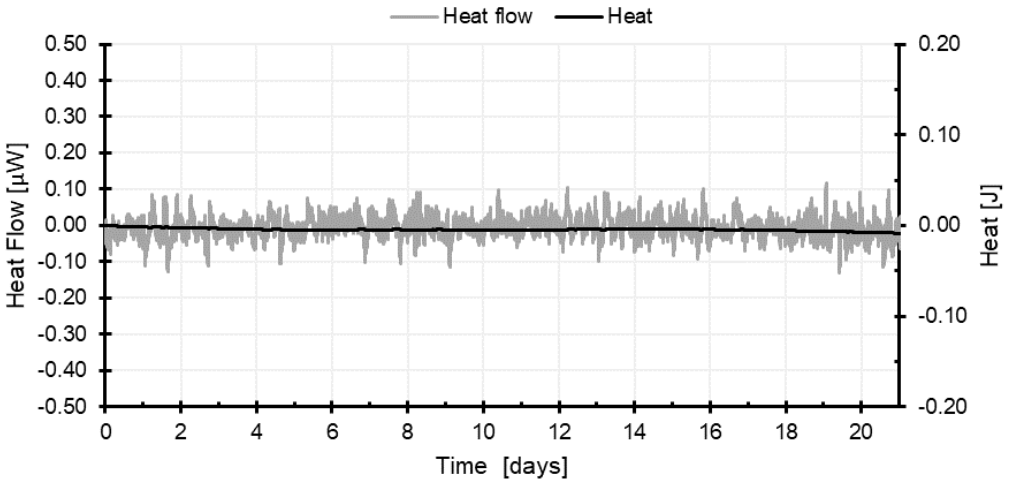

Figure 43. Heat flow and heat for one of the microcalorimeters installed in TAM III

Calibration of TAM III

The calibration of the MC is carried out using a built-in mechanism in the MC (electrical microwatt heaters) to obtain a correction factor and the heat flow results are corrected by the software. But in order to have better understanding and confidence in the results, the MC was calibrated using 4 g standard reference materials known as sapphire and the specific heat (Cp) obtained over a range 20-65 °C, was compared with that from the NIST database. The factor obtained after dividing the Cp of sapphire from the NIST data with that from the MC run was then compared and the results are shown in Figure 44.

Measurement uncertainties

The correction factors from the calibration of both MC channels were 0.98 for the 1st channel and 1.002 for the 2nd channel. Hence, the measurement uncertainties are surprisingly low and support the findings that the MC technique can be used to measure the thermal properties in polymeric materials for example.

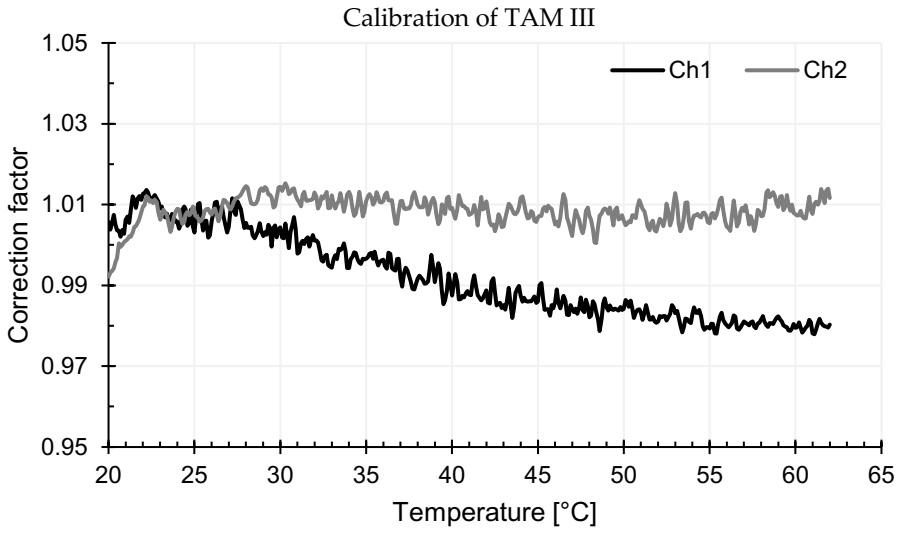

Figure 44. Correction factor for two different channels in microcalorimeter over 25-62 °C.

7.2.3 Determination of the activation energy using MC results

The temperature dependence of a reaction rate (k) can be studied assuming it follows the Arrhenius equation (7), and the kinetic parameters can be calculated using MC data. Multiplying heat of the reaction Q (J/g) on both sides of the equation (7) and by taking natural logarithm represents an equation of a straight-line equation 8. If the process shows a constant rate of reaction at each temperature in the isothermal mode, the activation energy can be calculated from an Arrhenius plot of ln (thermal power) as a function of $1/T$ (T in kelvin). However, if the thermal power is changing during the measurements, i.e., the reaction rate is influenced by the extent of the reaction during the experiment, the activation energy should then be calculated using the thermal power measured at the same extent of reaction at the different temperatures. The extent of reaction is proportional to the heat of the reaction, so the Arrhenius plot can be made with thermal power assessed at the same amount of produced heat. To obtain the kinetic parameters, thermal power needs to be measured at a minimum of three different temperatures. A curve for ln versus $1000/T$, can be obtained by a linear fit of the data. Activation energy, E (kJ/mol), is obtained from the slope of the linear fit,

which is equal to $-E/R$. QA (J/kg s) is obtained by taking the exponential of the intercept on the y-axis at time zero (see equation 8).

[7]

[8]

where R is the universal gas constant, 8.314 J/(mol K), Q is the heat of reaction, J/kg and A is the rate constant (s^{-1}).

7.2.4 Results

A MC test result for model or grade 1 material and Tremco sealing is shown in the Figure 45. The normalized heat flow (thermal power) was measured for about 25 days. The normalised heat flow for grade 1 material as expected has shown a constant value around 2 μW/g and the measured heat flow is in good agreement with the MC test conducted using same material in 2021 (normalised heat flow was 1 μW/g). This shows that result for grade 1 is reproducible and difference of 1 μW/g (is expected) is most likely within uncertainty by MC and may be the inhomogeneity in the sample. The normalised heat flow for Tremco sealing was almost double, that is around 4 μW/g for about 430 hours and then a step increase in the heat flow can be observed. The normalised heat flow after 430 hours remained significantly higher. In principle positive values of heat flow as measured for both the materials is an indication of exothermic processes and most likely be the oxidation. The Tremco sealing was oxidising at significantly higher rate that grade 1 material. The reasons for what was oxidising in the Tremco sealing cannot be explained because recipe of not known however, oxidation is most likely the reason for exotherms (normalised heat flow) using Tremco sealing. A step-rise in the normalised heat flow after about 430 hour is an interesting phenomenon and need further investigation.

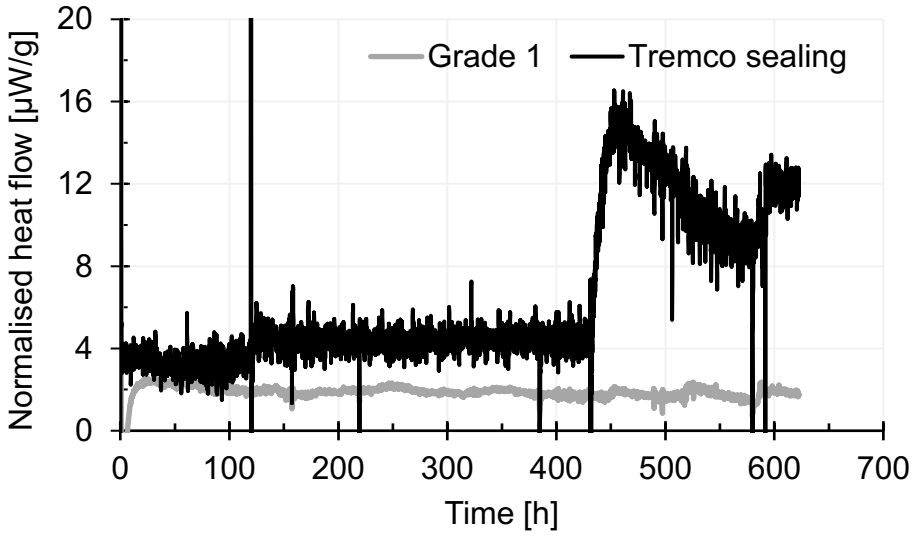

Figure 45. An Isothermal MC test at 90 °C using grade 1 and Tremco sealing.

Physical investigation of the material after MC test at 90 °C shows that the sample was deformed and significantly softened at 90 °C as shown in the Figure 46.

Figure 46. Tremco sealing after MC test at 90 °C.

This indicates that for the polymeric materials like Tremco sealing ageing at 90 °C was most likely harsh and should be avoided unless material may experience similar temperatures in NPP. The ageing test should be conducted closer to the real-life service conditions in NPP that is around 40-50 °C. Figure 47 shows the cross section of the Tremco sealing, with respected to the oxidised surface show in Figure 48, material was appeared to be at least significantly less oxidised from the inside (cf. Figure 47).

Figure 47. A cross section of Tremco sealing

Figure 48. The hardened surface of Tremco sealing.

Quasi-isothermal test using Tremco sealing

The normalised heat flow for a quasi-isothermal test is shown in Figure 49. Slow oxidisation (positive normalised heat flow on y-axis) can be seen at 70 °C. With respect to 70 °C, normalized heat flow at 80 °C, 90 °C and 100 °C are higher as expected and indicates oxidation in Tremco sealing. As presented above that Tremco sealing was soften and seemed like started melted after MC test at 90 °C. The quasi-isothermal test indicates that if in real service-life material may not experience higher than 50 °C, oxidative ageing should not be performed at higher temperatures for example higher than 50 °C. Normalised heat flow at 60 °C was endothermal (normalised heat flow is about 2 µW/g) and at least oxidation was below the detection limit of the instrument in a short time duration test (a day). The quasi-isothermal test shows that if there was oxidation at 50 °C, it was significantly slower than for example 90 °C.

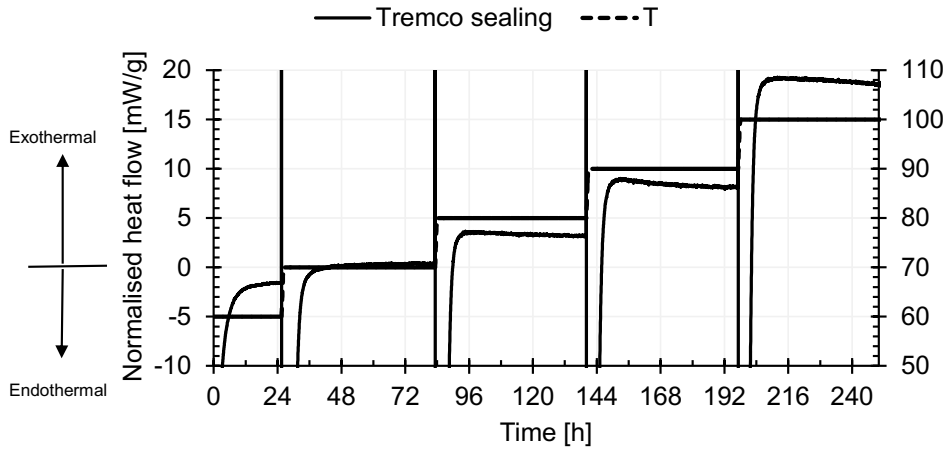

Figure 49. Normalised heat flow from a quasi-isothermal MC test at 60, 70, 80, 90 and 100 °C using Tremco sealing.

FTIR analysis of the Tremco sealing

FTIR analysis of the Tremco sealing was conducted from inside (cf. Figure 47 and Figure 48). The result for FTIR analysis is shown in Figure 50. As shown in the Figure 50 spectra between 3000-3300 cm-1 is most likely due to formation of hydroxyl groups which can occur from hydrolysis. This may have resulted into hardened surface however, inside material was still elastic.

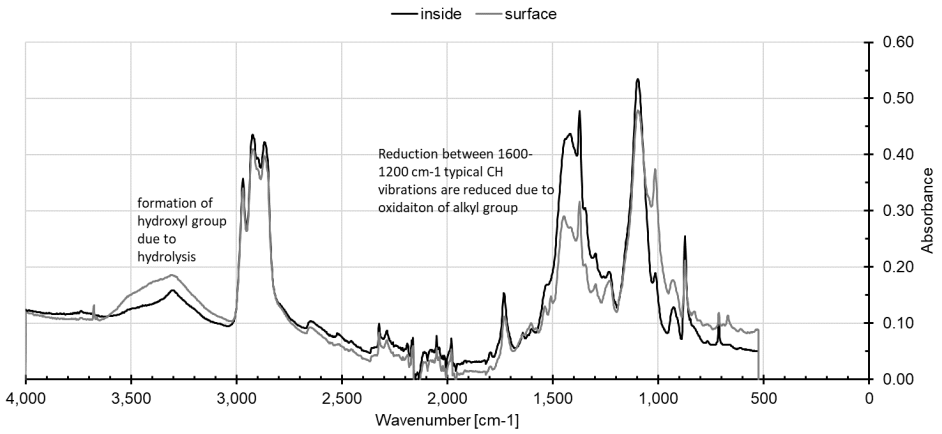

Figure 50. FTIR analysis of Tremco sealing from inside and oxidised surface.

7.2.5 Microcalorimeter and life-time prediction

Aim was to find how MC data can be used to obtain the lifetime of the material. A brief of what has been done is listed below.

- Activation energy using MC data for grade 1, 2 and 3 materials is compared with a widely accepted accelerated thermal ageing (ATA). The activation energies for different grades 1,2 and 3 were obtained previously and older version of the reports can be referred for detailed information.

The activation energies for different grades using MC and ATA data are presented in Table 5.

Table 5. Activation energy for different grades using MC and ATA.

Material	Activation energy KJ/mol	Temperature range	remarks
Grade 1, MC	81	80, 100 and 140 °C	
Grade 1, ATA	100	90, 120 and 140 °C	Using stress relaxation
Grade 2, MC	115±5	120 and 140 °C	
Grade 2, ATA	≈100 and ≈138	90, 120 and 140 °C	Using compression set and stress relaxation
Grade 3, MC	96±1	50, 60 and 70 °C	Temperature range is not same. Activation energy was obtained using stress relaxation
Grade 3, ATA stress relaxation	98	80, 90 and 100 °C	

Grade 1

Activation energy obtained using MC is listed in Table 5. Detailed information can be read in the manuscript or will be enclosed later after the acceptance of the manuscript (Pushp, Lönnermark et al. 2023). However, a summary of the findings is listed as below.

- Using MC it was possible to measure the thermal degradation in grade 1 material at 60 °C and above.
- Activation energies obtained at 60, 70, 80 °C (lower temperature) and 80, 100 and 140 °C (higher temperature), has shown different values. For example, activation energy at lower temperature was about 30 KJ/mol however at higher temperature it was about 81 KJ/mol. The activation energy obtained at higher temperature is not same as it was with ATA testing and ageing temperatures were not exactly same either. However, trend in the activation energy obtained using MC and ATA is same that is for grade 1 material activation energy is lower than for grade 2.
- An important finding after ageing in MC and post analysis of the EPDM material indicates that activation energy obtained closer to the service conditions that is around 60 °C is primarily due to the reactions by the peroxide system and antioxidant (Pushp, Lönnermark et al. 2023). No sign of oxidation of base polymers was seen at 60 °C. A mild oxidation was seen only after 120 °C (Pushp, Lönnermark et al. 2023).

Grade 2

Activation energy was obtained using MC at two different temperatures 120 and 140 °C. The selection of both temperatures was made, so, that data can be compared with ATA that was conducted at same temperatures (120 and 140 °C). The MC tests at 120 and 140 °C was conducted for about 1.5 weeks and the values of activation energy was obtained for same degree of conversion. Activation energy value obtained using MC are in reasonably good agreement with compression set and stress relaxation method. For better understanding of the changes in the material deeper investigation using alternate technique may be useful. The post analysis is not conducted in this study as it was beyond the scope of the project. The Arrhenius fit for two different degree of conversion is shown in the Figure 51.

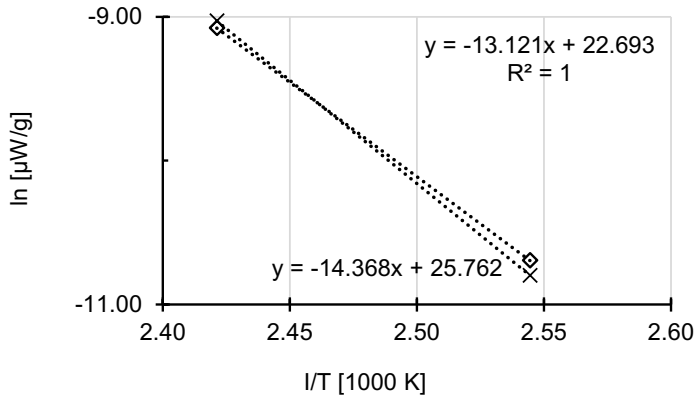

Figure 51. Activation energy for two different degree of conversion, 3 and 3.4 J/g at two different temperatures 120 and 140 °C.

Grade 3

Two different grade 3 materials were tested using MC. Arrhenius plot for both is shown in the Figure 52 and Figure 53. A straight line fit for both materials are reasonably in good agreement as all three points lying on straight line. The activation energy presented in Table 5 for MC, for example is obtained by multiplying slope from the Arrhenius fit that is 11.63 with the gas constant 8.314 J/K.mol, which has provided activation energy equals to 97-95 KJ/mol.

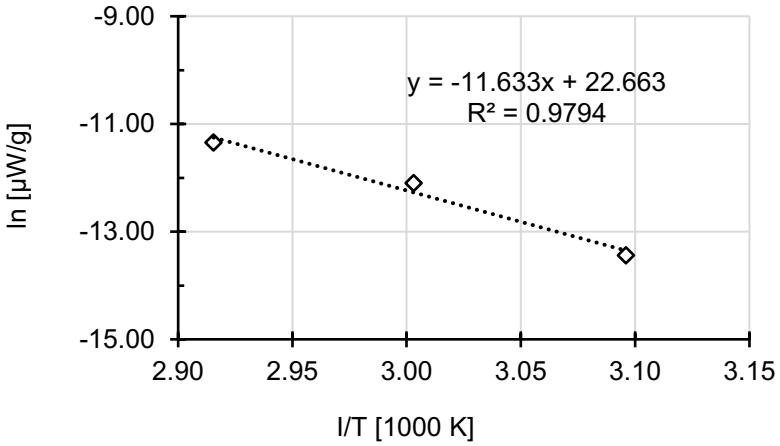

Figure 52. Arrhenius plot for commercial or grade 3 material.

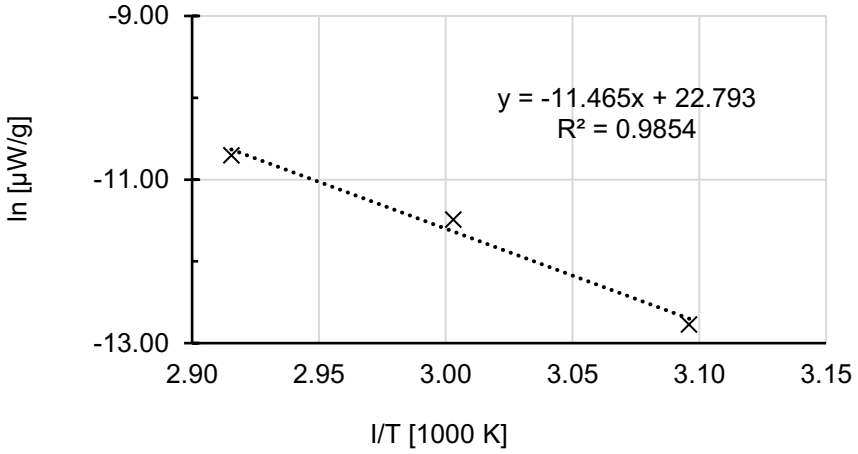

Figure 53. Arrhenius plot for commercial or grade 3 material with reinforcement.

NOTE: The activation energies obtained using MC and ATA techniques are matching within experimental error despite temperature range are different. Weather both techniques and difference in temperature range have same basis of comparison needs deeper investigation. For example, it is must to identify the chemical changes in the material and to related it with activation energies obtained at different temperature ranges or using different techniques.

7.2.6 Conclusions

Based on the MC tests and comparison with the ATA technique some conclusions can be drawn.

- MC can be used as a promising technique for the ageing tests closer to the service life of the polymeric material in NPP.
- Ageing tests can be conducted in real time and in significantly shorter duration for example 1 month activation energy can be obtained, post analysis of the polymeric material at least using standard techniques for example SEM-EDX and FTIR may provide valuable information about the ageing mechanisms.

8 References

Adhikary, M., Biswas A. and Akhtar M. J., "Active integrated antenna-based permittivity sensing tag." *IEEE sensors letters* 1.6 (2017): 1-4

Barthel, J. M. G. and Buchner, R., "High frequency permittivity and its use in the investigation of solution properties" Pure and Applied Chemistry, vol. 63, no. 10, (1991), pp. 1473-1482.

Burnay, S., "Degradation of Polymeric Components in Nuclear Power Applications" (2018), Energiforsk report 2018:480

Celina, M., Gillen, K. T. and Assink, R. A. (2005). "Accelerated aging and lifetime prediction: Review of non-Arrhenius behaviour due to two competing processes." Polymer Degradation and Stability 90(3): 395-404.

Daily, C. (2015). Dielectric properties and degradation monitoring in polymer-matrix structural composites. Grad. Theses Diss. https://doi.org/10.31274/etd-180810-3883

Forsström, D., Svensson, L.-G. and Terselius, B. (2000). "Thermo-oxidative stability of polyamide 6 films: III. Isothermal microcalorimetry." Polymer Degradation and Stability 67(2): 263-269.

Huang, H. (2015). Antenna Sensors in Passive Wireless Sensing Systems, in: Chen, Z.N. (Ed.), Handbook of Antenna Technologies. Springer Singapore, Singapore, pp. 1–34. https://doi.org/10.1007/978-981-4560-75-7_86-1

Li, L. (2011). Dielectric properties of aged polymers and nanocomposites (Doctor of Philosophy). Iowa State University, Digital Repository, Ames. https://doi.org/10.31274/etd-180810-1135

Nicolson, A. M. and Ross, G. F., "Measurement of the intrinsic properties of materials by time-domain techniques," IEEE Trans. Instrumentation and Measurement, 19, 377-382, (1970).

"Polymers in nuclear applications (2019)", Conference, November 27-28, Fortum head office, Keilalahdentie 2-4 (CD-building), Espoo, Finland.

Pushp, M., A. Lönnermark, P. Vikegard, X.-F. Wei and M. Hedenqvist (2023). "Ageing tests closer to real service conditions using hyper-sensitive microcalorimetry, a case study on EPDM rubber." Polymer Testing 120: 107948.

Rohde & Schwarz "Measurement of Dielectric Material Properties," Application Note RAC0607-0019_1_4E, (2012).

Sipilä, K., Vaari, J., Jansson, A., Bondeson, A. Condition monitoring, thermal and radiation degradation of polymers inside NPP containments (COMRADE), Report for COMRADE project (2018).

Weir, W. B., "Automatic measurement of complex dielectric constant and permeability at microwave frequencies," Proc. IEEE, 62, 33-36, (1974).

LIFETIME PREDICTION OF POLYMERS IN NUCLEAR POWER PLANTS 2022

Acceptance criteria, safety margins and aging management of polymer components are crucial to the safety and efficiency of Nordic nuclear power plants. The SAMPO project which ran from 2019 to 2023 as a collaboration between RISE and VTT aimed to address some of the challenges of prolonged service of polymer components.

RISE contribution is summarized in this report and contains results from four work packages of the project:

- Acceptance criteria and Safety margins for O-rings used in NPPs
- Improved estimation of service life of critical polymer components
- Online measurement to detect material degradation
- More sensitive analysing techniques

Ett nytt steg i energiforskningen

Forskningsföretaget Energiforsk initierar, samordnar och bedriver forskning och analys inom energiområdet samt sprider kunskap för att bidra till ett robust och hållbart energisystem. Energiforsk är ett politiskt neutralt och icke vinstutdelande aktiebolag som ägs av branschorganisationerna Energiföretagen Sverige och Energigas Sverige, det statliga affärsverket Svenska kraftnät, samt gas- och energiföretaget Nordion Energi. Läs mer på energiforsk.se.

Energiforsk